Airborne aerosols over central Africa during the Experiment for Regional Sources and Sinks of Oxidants (EXPRESSO)

Stéphane Ruellan, Hélène Cachier, Annie Gaudichet, Pierre Masclet, Jean-Pierre Lacaux

JOURNAL OF GEOPHYSICAL RESEARCH, VOL. 104, NO. D23, PAGES 30,673–30,690, DECEMBER 20, 1999

Airborne aerosols over central Africa during the Experiment for Regional Sources and Sinks of Oxidants (EXPRESSO)

Stéphane Ruellan,[1] Hélène Cachier,[1] Annie Gaudichet,[2]
Pierre Masclet,[3] and Jean-Pierre Lacaux[4]

Abstract. As part of the Experiment for Regional Sources and Sinks of Oxidants (EXPRESSO) conducted over central Africa in November 1996, 24 airborne aerosol samples were obtained and further analyzed for black and organic carbon (BC and OC), water-soluble organic carbon (WSOC), polycyclic aromatic hydrocarbons (PAHs), soluble ions, elemental composition, and morphology. Particles were collected in the different atmospheric layers either above the tropical forest or the savanna of central Africa near the Intertropical Convergence Zone. Particle number concentrations (10–14,000 nm diameter) were found to be high in all atmospheric layers (3100 ± 2060 cm^{-3}, $n = 24$). Soil-derived particles were less abundant than expected (20 ± 18 $\mu g\ m^{-3}$, $n = 21$), and their presence was assessed mainly to reentrainment by fires. On the other hand, pyrogenic particles were abundant, and high levels of black carbon (BC) concentrations were found either in the forest boundary layer (3.8 ± 2.3 $\mu g\ m^{-3}$, $n = 6$), the savanna boundary layer (9.8 ± 3.9 $\mu g\ m^{-3}$, $n = 6$), or in the Harmattan layer (8.7 ± 1.6 $\mu g\ m^{-3}$, $n = 3$). Other fire tracers (such as K, oxalate, or PAHs) confirmed the overwhelming impact of savanna fires in the regional troposphere. Another result is the possible occurrence of vertical and horizontal exchanges between the different layers and through the ITCZ. WSOC was measured in our samples representing on average 46 ± 9% ($n = 11$) of the total particulate organic carbon. High values were found in the Harmattan layer, where on average WSOC accounts for 85 ± 18%, ($n = 3$) of the total particulate organic carbon, pointing out the potential of biomass burning particles to act as cloud condensation nuclei (CCN). Different chemical indicators were used, which produce convergent information on the aging of biomass burning particles. Among these indicators, the ratio WSOC/OC was found to increase by a factor of 2 to 3 from the ground to the Harmattan layer. A product of this work is also the presence of high concentrations of organic acids (formate, acetate, and also oxalate) in the forest boundary layer suggesting a strong biogenic source for these compounds. Finally, during the EXPRESSO experiment, which took place at the beginning of the dry season, savanna fires were prevailing at a regional scale, whereas dust inputs by Harmattan airflow were still low. Our results suggest that in these conditions nitrate primarily remains in the gaseous phase, and thus the translocation of nitrogen nutrients is confined to the region.

1. Introduction

Previous studies have underlined the potential for biomass burning gases and particles to perturb the tropical atmosphere [*Levine*, 1991; *Cachier*, 1992; *Crutzen and Andreae*, 1990]. Atmospheric pollution is at maximum during the dry season when savanna or forest fires occur on a regional scale. Africa is particularly affected by this phenomenon due to the areal extension of the savanna zones. The contribution of African savanna fires has been estimated to account for 30% of global biomass burning emissions of trace gas and aerosols [*Lacaux et al.*, 1993]. Thus, since the last decade, several experiments have been conducted on this continent in order to characterize the emissions both on a qualitative and quantitative point of view. Consistent results were obtained during large international projects such as Dynamique et Chimie Atmosphérique en Forêt Equatoriale (DECAFE) in the Ivory Coast and Congo [*Lacaux et al.*, 1995] or Transport and Atmospheric Chemistry Near the Equator—Atlantic/Southern African Fire-Atmosphere Research Initiative (TRACE—A/SAFARI) in South Africa and Brazilian cerrado [*Andreae et al.*, 1994]. They pointed out the overwhelming influence on a continental scale of biomass burning pollutants extending from source regions in the oceanic atmosphere. Tropical savanna biomass burning aerosols have been chemically characterized primarily at ground level close to sources, and for various species, fluxes were evaluated [*Cachier et al.*, 1995; *Gaudichet et al.*, 1995; *Masclet et al.*, 1995]. Airborne aerosol measurements performed during the TRACE—A experiment [*Anderson et al.*, 1996] or ground-level measurements conducted at remote oceanic sites [*Cachier et al.*, 1996; *Swap et al.*, 1996] have also shown that pyrogenic particles emitted on the African conti-

[1]Laboratoire des Sciences du Climat et de l'Environnement, CNRS, Gif sur Yvette, France.
[2]Laboratoire Interuniversitaire des Sciences de l'Atmosphère, Faculté de Sciences, Université Paris XII, Cretéil, France.
[3]Laboratoire d'Etude des Systèmes Atmosphériques Multiphasiques, Université de Savoie, Le Bourget, France.
[4]Laboratoire d'Aérologie, Toulouse, France.

Paper number 1999JD900804.
0148-0227/99/1999JD900804$09.00

nent could undergo long-range transport over the remote Atlantic or Indian oceans. Particles are recognized to influence the radiative budget of the atmosphere either by direct or indirect effects [*Intergovernmental Panel on Climate Change (IPCC)*, 1995]. Owing to the seasonality of large-scale fires and the importance of emissions, biomass burning aerosols are expected to greatly affect the atmospheric radiative balance especially during the winter dry season.

The Experiment for Regional Sources and Sinks of Oxidants (EXPRESSO) took place in November 1996. This project was designed to investigate processes controlling the chemical composition of the tropical atmosphere over central Africa. At this period, savanna fires were already very numerous (as shown by fire pixels [*Grégoire et al.*, this issue; *Pereira et al.*, this issue], although the onset of the dry season was still underway especially in the southernmost portion of the savanna zone of central Africa. The EXPRESSO experiment presented a unique opportunity for a better knowledge and understanding of the level of concentration and chemical behavior of biomass burning aerosols in the different atmospheric layers. An important issue has been to evidence particle transformations due to aging processes. Thus consequences on the biomass burning aerosol signature have also been investigated.

In this paper we present a speciation of the particulate phase which shows the overwhelming contribution of fire-derived aerosols. Our data give some insight into the important aging processes affecting the particles by comparing their physical and chemical characteristics in the different layers. For this purpose, morphological studies were undertaken, and the inorganic, organic, and black carbon particulate fractions were analyzed. The water-soluble component of the carbonaceous fraction was also evaluated as biomass burning organic particles are suspected to serve as cloud condensation nuclei (CCN) agents [*Novakov and Corrigan*, 1996; *Hudson et al.*, 1991; *Dinh et al.*, 1994]. An interesting output of our data is also the distribution of aerosols in the regional atmosphere, which, in another paper currently underway, will be compared to that obtained by mesoscale modeling of particulates estimated to have been emitted by fires during the experiment.

2. Experiment

2.1. Onboard Instrumentation and Sample Collection Strategy

The French aircraft Avion de Recherche Atmosphérique et de Télédétection (ARAT) used during the experiment is a Fokker 27. In tropical conditions and once the scientific equipment was installed, the endurance was about 2 hours. A central acquisition system (SAcCADe, Unit A900) gathered all the data measured onboard. For the purpose of this work, we used continuous measurements of the geographical position (Sercel Global Positioning System (GPS)), altitude (ground altimeter, TRT AHV12), static pressure (Rosemount 1201 F1), the dew point temperature (General Eastern 1011B), and its product, the water vapor mixing ratio. Real-time counting of particles was performed with a Thermo Systems Inc. (TSI) 3022 condensation nuclei counter, detecting particles (CN) with diameters between 10 and 14,000 nm, over the range of 10^{-2} to 10^{7} cm^{-3} at a constant flow rate of 5 cm^3 s^{-1}.

For the purpose of chemical measurements, aerosols were collected in parallel on filters with two independent lines running at 1 and 5 m^3 h^{-1} and respectively equipped with 0.8 μm Nuclepore© membranes and either GF/C Whatman© glass-fiber filters or Pallflex teflon filters for the second line. These lines were fitted on an external inlet pointing into the oncoming airstream and designed to assure isokinetical conditions for the prescribed flow rates and aircraft velocities. Most of the filter samples were obtained during horizontal legs above savanna or forest areas. Sampling duration, ranging from 18 to 60 min, was chosen as a compromise between the analytical demand and the flight schedule. In order to remain in a given characterized atmospheric layer, the flight altitude was chosen from indications of several parameters such as the dew point temperature and the water vapor mixing ratio. The 11 flights (24 samples) started from Bangui (4°23°N, 18°34°E) and took place between 1030 and 1300 local time (UT + 1), south of the Intertropical Convergence Zone (ITCZ) ground location. A description of all the collected samples (positions, characteristics of the air mass, and analyses performed) is given in Table 1.

2.2. Analytical Methods

2.2.1. Carbon analyses. Solvent extracted GF/C glass-fiber filters were used for the purpose of carbon analysis [*Cachier et al.*, 1986]. This choice was dictated by our concern for the highest possible flow rate and for minimizing positive artifacts during samplings. The analytical protocol routinely applied in our laboratory [*Cachier et al.*, 1989] comprises a decarbonatation before carbon analysis. Black carbon (BC) and organic carbon (OC) are separated during a thermal pretreatment (340°C during 2 hours under oxygen). BC and TC (TC = OC + BC) are then determined on aliquots of the same filter by coulometric titration using a Ströhlein Coulomat 702C analyzer with a precision better than 10% for the samples analyzed here.

The particulate water-soluble organic carbon (WSOC) content was determined on portions (1/4) of Nuclepore membranes. The extraction and analysis of WSOC have been evaluated for their potential to bring contamination, which, in this procedure, may be important. Samples were sonicated during 5 min in 10 mL pure water (ELGA Maxima). Then, another 10 mL of water was added, and the membrane was removed. The 20 mL solution was immediately filtered on prewashed Nuclepore membranes (with a cutoff diameter of 0.2 μm), and the filtrate was analyzed for WSOC by using a Total Carbon Analyzer (TOC 700, O-I Analytical) and following the analytical protocol developed in our laboratory [*Pertuisot*, 1997]. In this protocol, 200 μL of ortho-phosphoric acid are added to the sample to remove the carbonates. Then 1 mL of sodium persulfate is added in the reactor heated at 100°C. Reaction time is prolonged to 15 min in order to oxidize all the organic species, and CO_2 is analyzed by IR. The instrument is calibrated with potassium biphtalate solutions. The reproducibility of measurements, including aliquot cutting, extraction procedure, and instrument variability was estimated to be better than 20%.

Pallflex teflon filters were used for polycyclic aromatic hydrocarbons (PAHs) determination. Filter cleaning consisted in soxhlet extraction with a 2/1 mixture of dichloromethane and cyclohexane. PAHs were extracted during 3 hours from the sample with the same mixture. The solvents were then evaporated under reduced pressure until the volume was 2 cm^3, and this fraction was filtered on sterile filters (cutoff 0.2 μm, Anotop 10 Plus). Before analysis, the sample was evaporated to dryness in a stream of nitrogen, then taken up again in 200 μL

Table 1. Sample Characteristics

Sample	Date	Altitude, m asl: Range	Altitude, m asl: Mean Level	ITCZ Ground Latitude	Mean Latitude	Mean Longitude	Water Vapor, g (water)/ kg (air)	Flight Location	Particle Analyses: BC + OC	PAH	WSOC	XRF	IC
43/01	Nov. 21, 1996	500–620	550	7°N	4.33	18.10	16.8	SBL	#	#	#	#	#
43/02	Nov. 21, 1996	880–1380	VP	7°N	4.35	18.08	16.4	SBL	#	#	#	#	#
44/01	Nov. 22, 1996	440–650	500	7°–8°N	4.73	18.33	16.1	SBL	#	#			
44/02	Nov. 22, 1996	940–1040	990	7°–8°N	4.71	18.32	16	SBL	#		#	#	#
45/01	Nov. 24, 1996	470–790	600	8°N	4.71	18.33	15.8	SBL	#	#	#	#	#
45/02	Nov. 24, 1996	2250–3310	3200	8°N	4.73	18.36	7.2	SH	#	#	#	#	#
46/01	Nov. 25, 1996	460–1060	500/1000	7°–8°N	3.31	17.92	16.9	FBL	#	#	#	#	#
46/02	Nov. 25, 1996	1930–4030	VP	7°–8°N	3.64	18.13	7.1	FH	#		#	#	#
47/01	Nov. 26, 1996	450–1060	650	7°–8°N	3.34	17.96	17.9	FBL		#	#	#	#
47/02	Nov. 26, 1996	2110–3830	VP/2600	7°–8°N	3.69	17.99	7.7	FH		#	#	#	#
48/01	Nov. 27, 1996	550–820	650	7°–8°N	5.35	19.24	14.7	SBL		#	#	#	#
48/02	Nov. 27, 1996	2520–2630	2600	7°–8°N	5.06	19.05	9.3	SH		#		#	#
49/01	Nov. 28, 1996	510–600	550	7°–8°N	3.45	17.98	16.4	FBL	#			#	#
49/02	Nov. 28, 1996	900–1330	1100	7°–8°N	3.65	17.97	13.8	FBL	#		#	#	#
50/01	Nov. 29, 1996	2430–3300	VP/3300	7°–8°N	3.33	17.50	7.2	FH		#	#	#	#
50/02	Nov. 29, 1996	1010–1200	1150	7°–8°N	3.26	17.45	15.5	FBL		#	#	#	#
51/01	Nov. 30, 1996	450–680	550	6°–7°N	4.72	18.33	10	SBL		#	#	#	#
51/02	Nov. 30, 1996	1070–1510	1400	6°–7°N	4.73	18.34	10	SBL		#	#	#	#
51/03	Nov. 30, 1996	2520–3620	VP	6°–7°N	4.61	18.39	6.5	SH		#	#	#	#
52/01	Dec. 1, 1996	500–600	550	6°N	3.70	18.21	16.8	FBL	#		#	#	#
52/02	Dec. 1, 1996	430–940	600	6°N	3.13	17.81	17.3	FBL	#		#	#	#
52/03	Dec. 1, 1996	1910–3950	VP/2700	6°N	3.80	18.07	5.8	FH	#				#
53/01	Dec. 2, 1996	1390–1650	1600	4°–5°N	3.61	18.06	14	FBL	#				
53/02	Dec. 2, 1996	460–1190	550	4°–5°N	4.62	18.30	15.7	SBL	#		#	#	#

VP, vertical profile; XXX, altitude of plateau in meters; BL, boundary layer; H, Harmattan layer; S, savanna; F, forest; ITCZ, Intertropical Convergence Zone; BC, black carbon; OC, organic carbon; WSOC, particulate water-soluble organic carbon; PAH, particulate polycyclic aromatic hydrocarbons; XRF, X-ray fluorescence; IC, ion chromatography.

ultrapure methanol. Analyses were performed by reversed phase high performance liquid chromatography (HPLC) on a Vydac C18 column. A Spectra Physics 8100 chromatograph was coupled to a Perkin Elmer F 1000 fluorimetric detector. A ternary elution gradient consisting of water, acetonitrile, and methanol was used to separate the different PAHs. The different species were identified and measured by UV fluorescence at variable excitation and emission wavelengths. Eight pairs of wavelengths were used in order to obtain the best possible selectivity and sensitivity. PAHs were quantified by internal calibration with a solution of triphenylene and dibenzo(ah)anthracene, two PAH species which are not present in the atmosphere. Thirteen PAHs were quantitatively determined: phenanthrene, anthracene, fluoranthene, pyrene, chrysene, benzo(a)anthracene, benzo(b)fluoranthene, benzo(k)fluoranthene, benzo(a)pyrene, benzo(e)pyrene, benzo(ghi)perylene, coronene, and retene. The reproducibility of measurements is in the range of 5 to 12% depending on the abundance of compounds in our samples.

2.2.2. Elemental analyses and microscopy observations. Nuclepore membranes were used for nondestructive analysis by wavelength dispersive X-ray Fluorescence (XRF) spectrometer. The XRF analysis was performed using a SIEMENS SRS 303 spectrometer with a rhodium primary X-ray tube. For the following elements analyzed: Al, P, S, Cl, K, Ca, and Fe, we only took into consideration samples for which we obtained a reproducibility better than 10%. For the purpose of microscopic observations, particles collected on the same membrane were transferred directly onto copper grids by dissolving the membrane substrate with filtered chloroform [*Gaudichet et al.*, 1986]. These grids were then introduced in a Transmission Electron Microscope (JEOL 100C) fitted with a microanalysis system (Energy Dispersive of X Rays, Tracor 5400). This fitting allows routine observation of single particles as small as 10 nm, as well as their morphological features, size, crystallographic properties, and elemental composition (for elements with $Z > 6$). Size of microsoot particles was measured at 19,000 magnification using a calibrated graticule.

2.2.3. Particulate ions. Anions and cations were extracted from aliquots of Nuclepore membranes by 15 min sonication in 15 mL ultrapure water. Ion analysis (sodium, ammonium, potassium, magnesium, calcium, chlorine, nitrate, sulfate, formate and acetate, oxalate) was then performed by ion chromatography (IC) using DIONEX QIC and DX 100 settings. International certified standards were used to calibrate mineral ions (references: 2694a.I SPIN for anions and 2694a.II SPIN for cations). The ion chromatography system used in this study and the main characteristics of the analytical parameters (columns, Eluant composition and rate, standards, and calibration, as well as chromatogram analysis) are described in detail by [*Galy-Lacaux and Modi*, 1998]. Analytical precision is estimated to be better than 5%.

3. Vertical Structure of the Atmosphere and Aerosol Number Concentrations

Gradient profiles of potential temperature, water vapor mixing ratio, and wind speed (Figures 1a and 1b) were used to retrieve the coarse structure of the atmosphere described in more detail by C. Delon et al. (unpublished manuscript, 1999). Above both savanna and forest regions, during the flights, the bottom part of the boundary layer was generally found to be unstable, showing that the development of the boundary layer was not totally achieved. The portion above 100 or 200 m

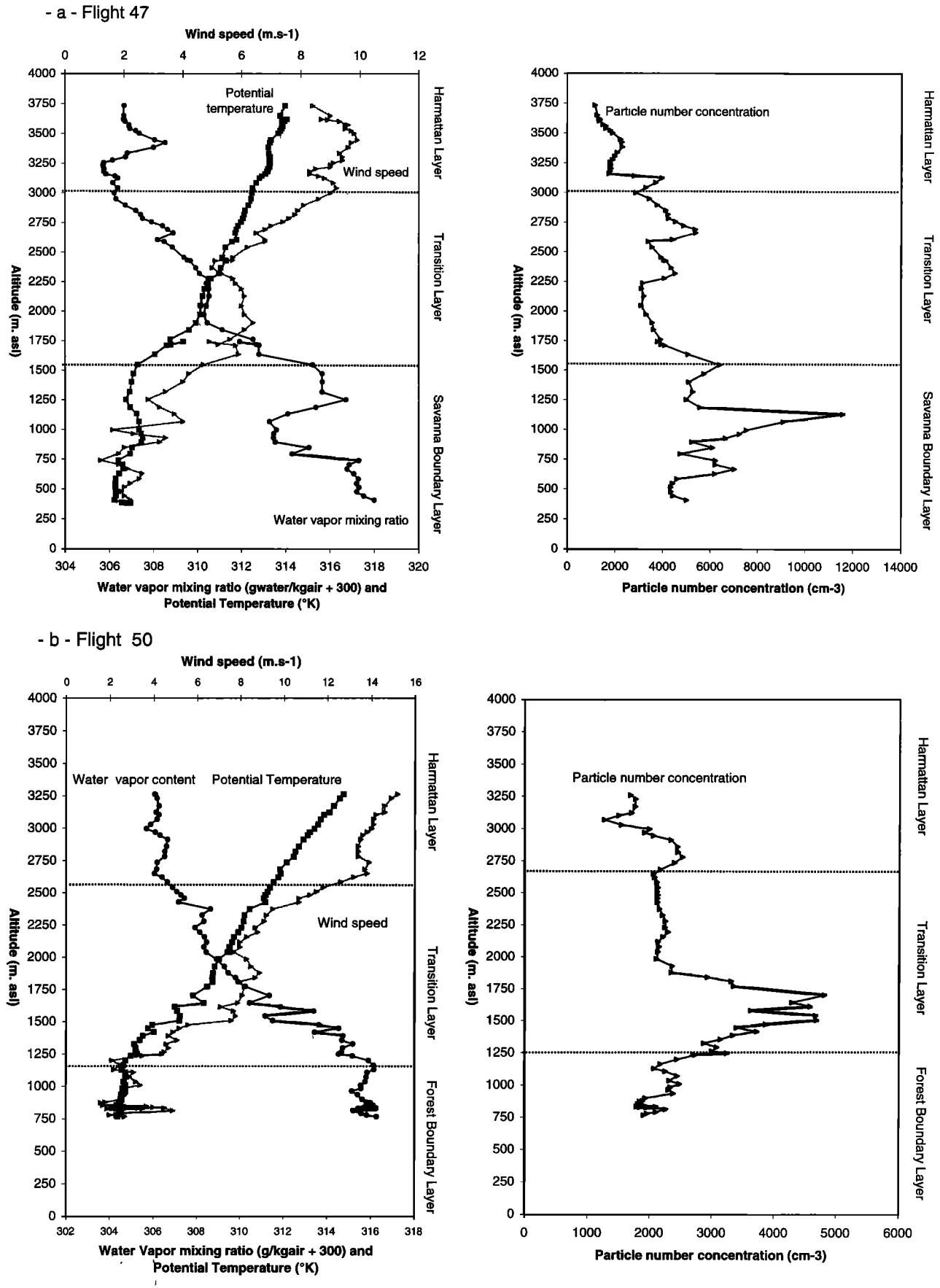

Figure 1. Use of potential temperature, water vapor mixing ratio, and wind speed vertical profiles to determine the three main atmospheric layers, and corresponding particle number concentration: (a) savanna (flight 47); (b) forest (flight 50).

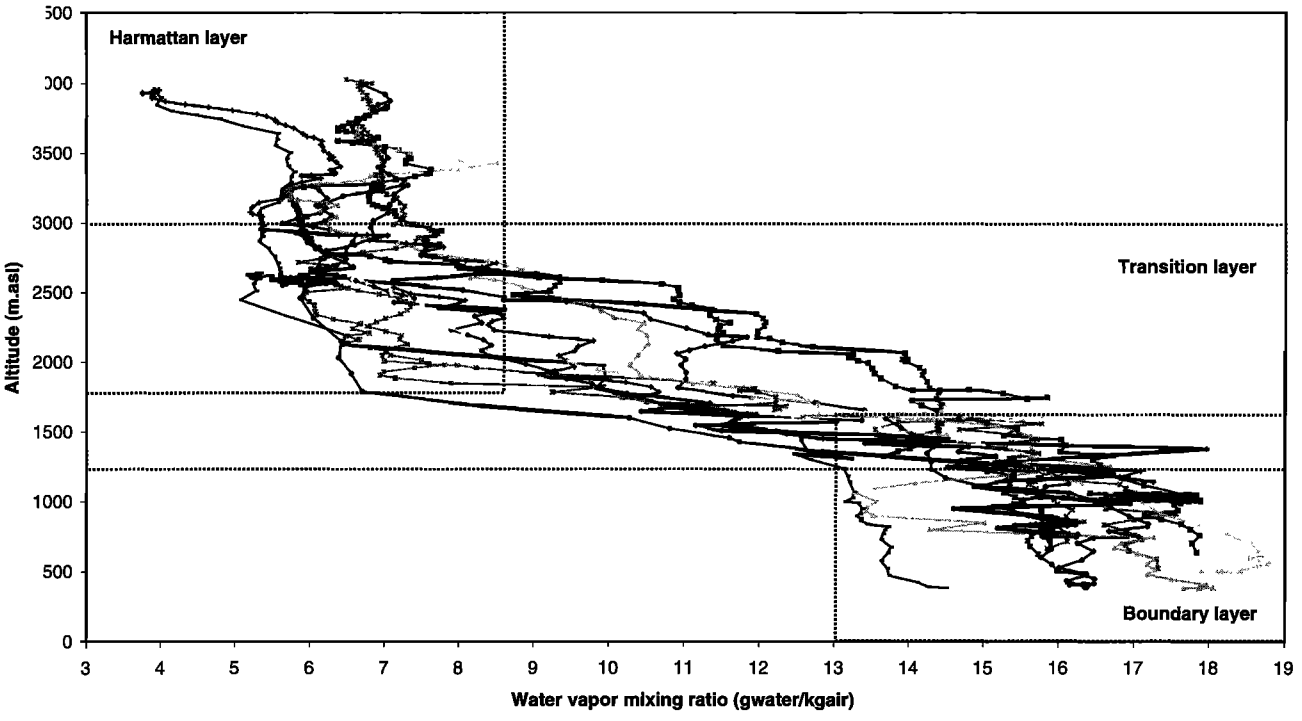

Figure 2. Tropospheric vertical profiles of water vapor mixing ratio obtained during EXPRESSO experiment: dry air is found in the Harmattan layer (water <9 g_{water}/kg_{air}), whereas the boundary layer is characterized by more humid air (water >13 g_{water}/kg_{air}).

(aboveground), up to the top of the boundary layer was often steady or slightly stable. The upper layer was always characterized by a more stable structure. Wind analysis showed that this layer was under the influence of Harmattan winds coming from northeastern regions. Most of the time these two layers were separated by a very stable intermediate layer showing a sharp negative water vapor gradient. The width of this transition layer was variable but often several hundred meters thick (Figure 2).

Filter sampling levels were chosen primarily either in the boundary layer (BL) or in the Harmattan layer (HL). The Monsoon or Harmattan origin of the sampled air mass was assessed easily from the mean water vapor mixing ratio recorded during the flights. For most of our samples, a clear cut was observed with this indicator ranging from 13.8 to 17.9 g_{water}/kg_{air} for the humid Monsoon air and from 5.8 to 7.7 g_{water}/kg_{air} for the dry Harmattan air of saharian origin. Nevertheless, three samples (48/02, 51/01, and 51/02) very close to the Intertropical Convergence Zone (ITCZ) displayed intermediate values of water vapor mixing ratio (around 10 g_{water}/kg_{air}) and could not be considered as pure Monsoon or Harmattan samples (Table 1).

In the savanna boundary layer (SBL), particle number concentrations obtained in real time were found in the range 500–6000 cm^{-3} with a mean value of 3700 ± 1500 (n = 9). The vicinity and great number of fires during EXPRESSO may explain these quite high values. The SBL profiles are also generally very noisy (20% of the total particle number concentration is attributed to CN noise peak) probably due to the presence of numerous point sources. Harmattan layers either above the forest or above the savanna appear much more homogeneous with on average, although still significant, lower particle number concentrations (2500 ± 1500 cm^{-3}; n = 7). In the forest boundary layer (FBL) the particle concentration values ranging from 200 to 3100 cm^{-3} (mean equal to 1600 ± 1300 cm^{-3}; n = 8) are lower. These values are much lower than those found by *Clairac et al.* [1988] inside the Mayombe forest of southern Congo (5000 cm^{-3}). The difference could be due to the presence of ultrafine (below 10 nm) biogenic particles, which were measured by these authors and not taken into account by our instrument. However, the coagulation of biogenic particles occurring rapidly above the canopy could also explain the discrepancy between the two experiments. CN peaks seen during the flat FBL profiles are very few since only 5% of the total particle number concentration can be attributed to noise peaks. Peaks often correspond to a potential temperature inversion which probably creates accumulation zone for aerosols as observed previously above Amazonia [*Pereira et al.*, 1996].

FBL homogeneity points either to a large homogeneous source of biogenic aerosols and/or to diluted inputs of fire effluents transported off savanna region. An increase of particle load is also commonly observed in the transition layer (20% increase above the savanna and 40% above the forest) where particles tend to accumulate, trapped by the strong dynamical stability prevailing in this upper part of the BL (Figures 1a and 1b). This layer could also be a location of sizeable vertical exchanges of aerosols by entrainment between the BL and the HL as suggested by the atypical values of water vapor mixing ratio. Recalling the relatively high values of particles in the HL over the forest, it is suggested that long-range transported particles may notably influence all the tropospheric layers over the forest. Such exchanges between the different layers were also shown by modeling [*Cautenet et al.*, this issue].

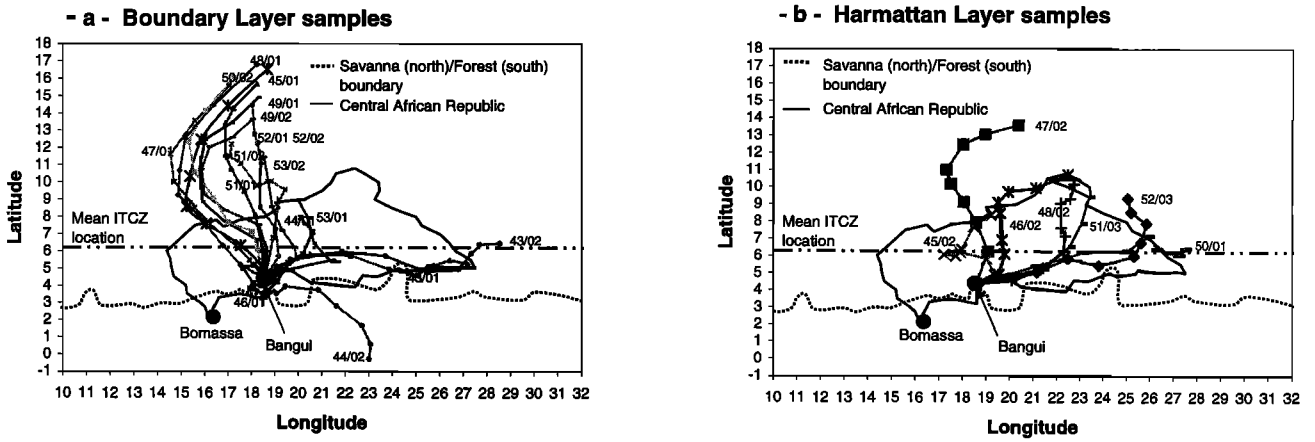

Figure 3. Back trajectories for samples in (a) the boundary layer and (b) the Harmattan layer using ECMWF data.

4. Air Parcel Back Trajectories

The origin and history of air masses sampled during the experiment was investigated from 4-day back trajectories, calculated from European Centre for Medium-Range Weather Forecasts (ECMWF) data. The product was three-dimensional isentropic back trajectories ending over Bangui (4°23°N, 18°34°E) at different atmospheric levels (1000, 925, 850, 700, and 500 hPa). We used the level corresponding to the flight altitude (mostly 925 hPa for BL samples or 700 hPa for HL samples) and presented them with a time step of 12 hours (Figures 3a and 3b). As expected, the highest altitude flights are influenced by airflow entrained by prevailing Harmattan winds. Most of the BL samples were also found to be affected by air masses coming from the north (southern and central Chad). Bangui being located south of the ITCZ, this result may suggest that air masses were able to cross the ITCZ. Thus import of pollutants from the savanna region to the uninhabited forested areas could explain the notable particle number densities measured in the FBL. An interesting point is also given by the back trajectories vertical profiles. In Figure 4 it may be seen that almost all back trajectories corresponding to HL samples have a starting point at lower altitude, generally in the BL. This result strongly suggests that fires prevailing in the northern savanna regions influence the upper atmospheric layer over Bangui and the forest.

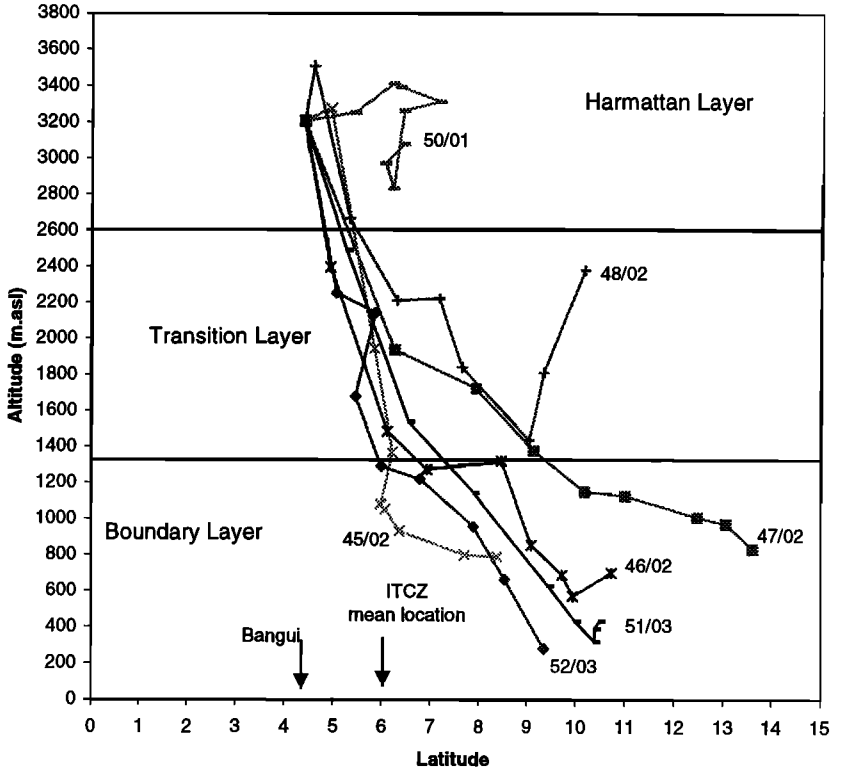

Figure 4. Vertical profile of air mass back trajectories calculated for Harmattan layer samples.

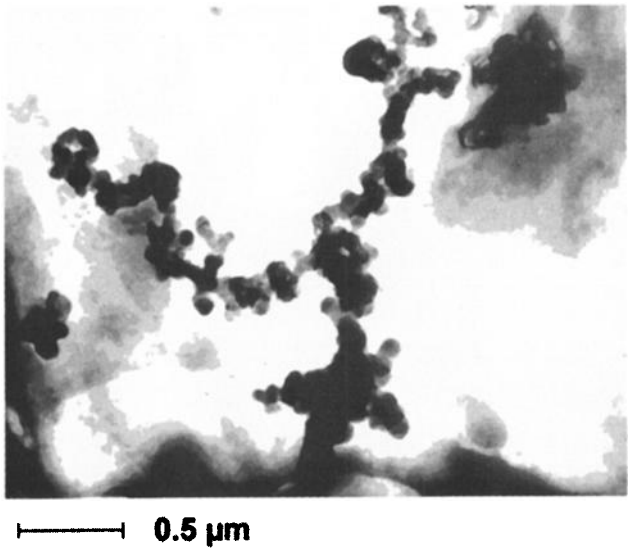

Figure 5. Transmission electron microscope picture of biomass burning particles (sample 45/01): chains and grapes.

5. Aerosol Speciation

In order to evaluate the relative impact of the different aerosol sources, microscopy observation of our samples was undergone prior to the quantitative analyses of the aerosols.

5.1. Microscopy Observation

Different types of particles were observed, either carbonaceous microsoots or inorganic particles. On each filter the most numerically abundant particles were microsoots. The biomass burning particles consist of submicron clusters of small carbonaceous spheres (≈20 nm diameter) appearing as elongated chains or more spherical aggregates (Figure 5). Each microsoot particle appears to be associated with potassium indicating unambiguously its typical biomass burning origin [*Cachier et al.*, 1991; *Gaudichet et al.*, 1995]. However, sulfur was also often found to be attached on microsoots. This unexpected result is confirmed by the bulk analysis of the aerosol showing high amounts of sulfur (sections 5.2 and 5.3).

Mineral particles consist of salt condensates and soil-dust-derived particles. Condensates are mostly submicron crystal sulfates linked both to Ca and K. According to their crystalline morphology and their composition they could only originate from biomass burning as previously observed [*Echalar et al.*, 1995]. Soil dusts are mainly clay species, such as Al, K, and Fe-containing illite or kaolinite.

5.2. Dusts

The total dust mass concentrations were calculated following *Bowen* [1966] with the mass ratio applied to aluminum (Al/dust = 7.1%). They were obtained from XRF analysis and are reported in Table 2. An average dust concentration of 20 ± 18 $\mu g\ m^{-3}$ (n = 21) was found with, as expected, differences from one layer to another. The highest values were found in the HL mostly influenced by air masses originating from northern regions. The SBL is characterized by intermediate values, and the lowest concentrations are encountered in the FBL. However, it must be noticed that dust concentrations above the forest are still much more important than those measured for aerosols sampled during the experiment inside the forest [*Roberts et al.*, 1998]. These results give evidence of dust inputs from northern latitudes which probably influence both the HL and the SBL but also the FBL which can exchange aerosols through the ITCZ and by subsidence from upper layers.

In the HL, dust concentrations are lower than expected, since they are lower than those measured during the dry season at Lamto savanna site (40 to 60 $\mu g\ m^{-3}$) [*Gaudichet et al.*, 1995] and comparable to those found off Africa in the oceanic atmosphere (Cape Verde) [*Chiapello et al.*, 1995]. The relatively poor influence of dust during EXPRESSO and the overwhelming importance of pyrogenic aerosols are underlined by the mass ratio of dust to total carbon in aerosols, which, on average, was lower than 40% for the different layers even in the upper troposphere. From Table 2 it appears that this ratio is minimum in the SBL where the impact of fires is maximum. The low dust concentrations combined with the prevailing

Table 2. Abundance in the Different Atmospheric Layers of Dust and Carbonaceous Particles

	Dust, $\mu g\ m^{-3}$	Tc, $\mu g\ m^{-3}$	BC, $\mu g\ m^{-3}$	Dust Abundance, %	K/Al Ratio	References
Savanna (ground level) (2)	6.5	14 ± 3	2.7 ± 0.5	37	1	this work
Savanna boundary layer (6)	21.4 ± 17.2	55 ± 30	9.8 ± 3.9	21.4 ± 9.7	1.0 ± 0.4	this work
Forest boundary layer (6)	13.6 ± 6.5	18.5 ± 5	3.8 ± 2.3	36.5 ± 13	1.16 ± 0.69	this work
Harmattan layer (5)	37.4 ± 36	42.2 ± 21	8.7 ± 1.6	39.2 ± 24	1.24 ± 0.71	this work
Lamto (Ivory Coast)	42–60	14.3 ± 3.7	3.4 ± 1.1	20 ± 4	0.4	*Cachier et al.* [1995] and *Gaudichet et al.* [1995]
Guinean savanna fires (11)						
Congo forest (ground level) (24)	2.7 ± 1	6.4 ± 2.3	1.7 ± 0.6	34 ± 13	···	*Roberts et al.* [1998] and this work
Amazonia burning season (Sept. 1992)	···	···	0.7–7.4	···	···	*Pereira et al.* [1996]
Forest and savanna fires, vertical profiles						
Amazonia burning season (Sept. 1995)	···	···	5.49	···	···	*Artaxo et al.* [1998]
Forest fires, airborne measurements						
Southern Congo forest (16)	···	6	···	···	···	*Clairac et al.* [1988]
Cape Verde Island (120)	20/45	···	···	···	0.18–0.24	*Chiapello et al.* [1995]
Nov./Dec. 1992–1994 (ground level)						

Values given are means and standard deviations. Here n is number of samples. BC, black carbon; TC, total carbon; OC, organic carbon = (TC − BC). OM = 1.3 × OC from *Brémond* [1989] and *Countess et al.* [1981]. Dust mass concentration derived from Al mass concentration, and the ratio Al/dust = 7.1% [*Bowen*, 1966]. Dust abundance is calculated as dust/(BC + OM). K/Al is used as an indicator of biomass burning inputs.

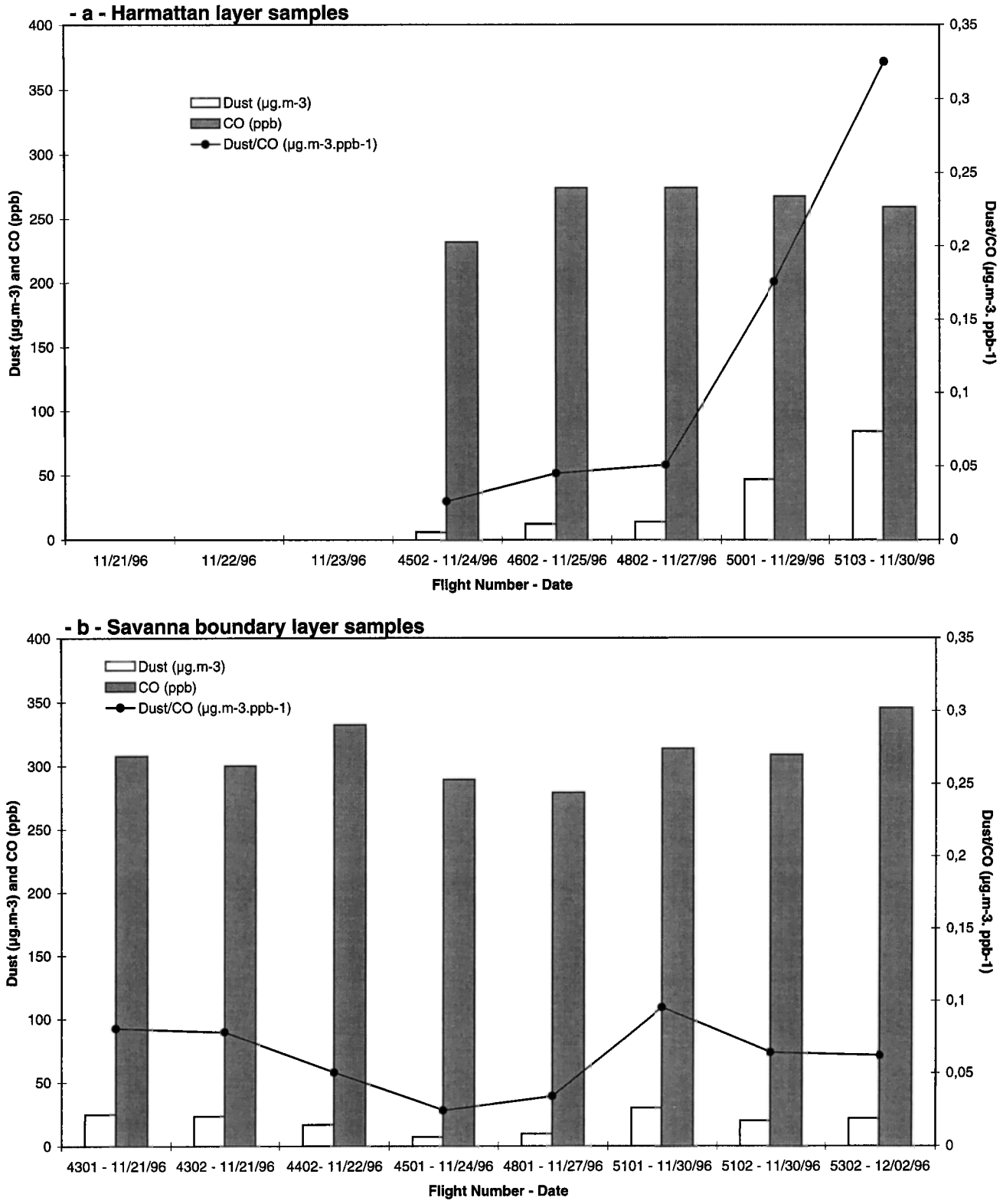

Figure 6. Evidence of dust entrainment by fires and from additional dust source in the Harmattan layer. CO is taken to normalize concentrations (C. Delon et al., unpublished manuscript, 1999). (a) Harmattan layer; (b) savanna boundary layer.

coarse mode of particles allow to assess that the terrigeneous contribution to the particle number concentrations (CN) is low compared to the contribution of biomass burning particles. Consequently, CN abundance will be used primarily as an indicator of biomass burning particles. Figure 6a represents throughout the whole experiment the evolution of dust concentrations in the HL and their enrichments by comparison to carbon monoxide which may be used as an indicator of fire

[*Hao et al.*, 1996]. Mean CO concentrations (266 ± 20 ppb, $n = 5$) are higher than the background values (100 ppb) obtained in the African tropical atmosphere [*Marenco et al.*, 1989], underlying the considerable influence of fires in the Harmattan layer. Throughout the experiment, the clear increase of both indicators (dust concentrations and dust/CO ratio) shows the growing influence of dust inputs during the onset of the dry season, whereas savanna fires probably remain at about the same state of development. In the SBL the dust/CO ratio is, however, rather constant all over the campaign (Figure 6b), and it may be suggested that for this layer the presence of dust is mostly due to the reentrainment by fires of soil particles previously deposited on the vegetation [*Gaudichet et al.*, 1995]. This hypothesis is reinforced by the good correlation ($r^2 = 0.8$) obtained between Al and K (usually associated with savanna fires [*Gaudichet et al.*, 1995; *Maenhaut et al.*, 1996; *Andreae et al.*, 1998]. In our samples the mean K/Al ratio of 1.1 ± 0.6 is higher than the crustal reference (0.2 [*Bowen*, 1966] and 0.3 [*Mason*, 1966]). This high value could confirm that K primarily originates from fires. Accordingly, among the HL samples, the most loaded with dust particles (50/01 and 51/03) display lower values of K/Al (0.5 and 0.7). The two SBL samples for which an incursion of dry Harmattan air was noticed (51/01 and 51/02) also exhibit lower values of K/Al (0.7 and 0.4). These results confirm the dual origin of potassium (fires and dust) in our samples. Even in the FBL, the K/Al ratio is similar to that observed for SBL aerosols, which suggests that additional biogenic inputs of K-enriched biogenic aerosols are not very important over the forest. It is also interesting to notice that the Fe/Al ratio is very constant (0.34 ± 0.05, $n = 18$) all over the campaign. This ratio is similar to the Fe/Al ratio (0.42) previously measured in northern Nigerian Harmattan dusts [*Moberg et al.*, 1991], but lower than the crustal references usually quoted in the literature (0.54 [*Bowen*, 1966] or 0.62 [*Mason*, 1966]). An exception is found for three samples (43/01, 43/02, and 50/01) for which Fe/Al is higher (0.57 ± 0.05, $n = 3$). Figures 3a and 3b show that, contrarily to the others (mainly affected by air masses coming from the north), these three samples were affected by air masses coming from east Sudan. This result suggests that the increase of the Fe/Al ratio could be due to an additional contribution of eastern sources for which Fe/Al is higher (0.9 average value of six local soils in eastern Gezira [*Penkett et al.*, 1979]). It is thus probable that during most of the EXPRESSO experiment, in all layers, air masses were homogeneously influenced by the same dust source region.

5.3. Carbonaceous Aerosols

As shown in Table 2, black carbon and total carbon concentrations obtained in each layer are extremely high, the highest ever reported in the tropical atmosphere (see references in Table 2). This result points to the importance of large-scale fires even in the early dry season and their overwhelming influence in a great portion of the global troposphere over Africa. The presence of numerous burning scars during the EXPRESSO campaign on both sides of the ITCZ [*Grégoire et al.*, this issue; *Pereira et al.*, this issue] may explain these high concentrations. BC concentration averages obtained in the SBL (9.8 ± 3.9 $\mu g\ m^{-3}$, $n = 6$) and the HL (8.7 ± 1.6 $\mu g\ m^{-3}$, $n = 3$) are still higher than the maximum mean value (7.4 $\mu g\ m^{-3}$) obtained during an airborne campaign above Amazonia where numerous forest or savanna fires were detected all over the Amazon forest [*Pereira et al.*, 1996]. Airborne values of carbonaceous particle concentrations are also about 3 times higher than the background concentrations obtained at ground level during the experiment or in the Ivory Coast during the fire season. As the experiment took place at the beginning of the burning season in central Africa, these results suggest that pyrogenic aerosol concentrations could have reached even higher values during the following weeks. In the SBL the vicinity of fires is observable as numerous particle peaks in the CN data. In the SBL, black carbon concentration of samples is also variable in time and space, whereas the HL appears to be more homogeneous with less CN peaks during each sample collection and a smaller BC variability from one sample to another, reflecting probably well mixed older plumes. In the FBL, carbon concentrations are lower which is consistent with the location of the main fire zones. Nevertheless, these FBL values are higher than expected, and they are also higher than those found at the top of the tower of Bomassa (Congo forest) during the same period (1.7 ± 0.6 $\mu g\ m^{-3}$) or in 1983 in the Mayombe forest [*Clairac et al.*, 1988]. During EXPRESSO the BL over the forest thus appears to be heavily influenced by savanna fires. Different factors may explain this result. First, during this period, an important number of fire pixels and burning scars was commonly observed south of the ITCZ ground position in the forested savanna. Second, as previously quoted, exchanges between the different atmospheric layers may occur as downward entrainment of pyrogenic material from the heavily loaded HL or horizontal exchanges through the ITCZ. This hypothesis is reinforced by the general southward direction of air mass trajectories (Figure 3a), suggesting an impregnation of the regional boundary layer by fires occurring in the savanna zone. The forest sample 46/01 may be considered as the most representative sample of the FBL. It displays the lowest BC (1.1 $\mu g\ m^{-3}$) and TC (14.6 $\mu g\ m^{-3}$) values which can be explained by the northward trajectory of airflow.

Potassium and in a less extent sulfur are usually associated with savanna burning particulate emissions [*Echalar et al.*, 1995; *Andreae et al.*, 1998]. Their presence has been previously observed on microsoots (section 5.1). In our samples, K and S display a satisfactory correlation ($r^2 = 0.77$). Moreover, K/BC and S/BC ratios are similar to those found in the background of Lamto. All these results are consistent with the sign of a biomass burning aerosol as a driver of K and S particulate contents in the atmosphere.

Oxidants formed by photochemistry (O_3, OH, NO_3) may react either with volatile organic compounds (VOC) or primary organic aerosols and generate various new organic functionalities containing alcohols, carbonyls, carboxylic acids, and more complex oxidized products [*Grosjean*, 1992; *Saxena and Hildemann*, 1996]. Most of these compounds are likely to be polar and can thus increase the water solubility of particles. Measurement of the particulate water-soluble organic content (WSOC) was performed on all the Nuclepore samples (Table 1). The relative importance of WSOC in the organic aerosols may be presented as the percentage WSOC/OC, found to be 46 ± 9% ($n = 11$) on average in our samples. For a matter of comparison with other works, we also calculated the WSOC/TC ratio. For our samples this ratio was found to be within a wider range (11 to 70%), and on average 31 ± 16% ($n = 11$), than values found in urban sites (from 20 to 55%) [*Cadle and Groblicki*, 1982; *Sempéré and Kawamura*, 1994; *Zappoli et al.*, 1999]. The ratio WSOC/OC is higher in the Harmattan layer (85 ± 18%, $n = 3$) than in the BL, and this

Table 3. PAHs Concentrations in Each Layer

PAHs	pg m^{-3}	PHE	ANT	FLA	PYR	RET	BaA	CHR	BeP	BbF	BkF	BaP	BghiP	COR	ΣPAH	ΣPAH/BC, %	ΣPAH/OC, %
SBL (5)	Mean	554	15	432	108	90	19	145	19	87	44	25	48	32	1055	0.008	0.0025
	s.d.	251	28	184	208	92	13	131	20	36	37	21	31	17	761	0.004	0.0013
FBL (3)	Mean	1106	12	235	99	50	43	192	18	66	22	10	21	24	687	0.035	0.003
	s.d.	824	19	148	36	28	40	218	4	20	22	15	32	4	460	(1)	(1)
HL (5)	Mean	1580	18	1776	173	99	57	339	39	166	118	37	27	13	2688	0.005	0.004
	s.d.	616	16	191	90	219	24	95	19	118	54	12	23	20	4100	(1)	(1)
Lamto (3)	Mean	...	...	440	830	...	...	220	117	57	33	23	187	273	2180	0.12	...
	s.d.	...	...	75	95	...	...	26	21	15	12	6	15	21	113	0.04	...

Here n is number of samples; s.d., standard deviation; ΣPAH, sum of all PAHs (PHE, ANT, RET, and BaA excluded). Lamto data from *Masclet et al.* [1995].

evolution will be discussed further (section 6). The wide range found for the WSOC/OC ratio cannot reflect different organic carbon sources as biomass burning particles are overwhelmingly predominant. As a result, this variability is probably related to atmospheric transformation of OC. The conjunction of different factors may explain the presence of WSOC. The surface proper chemical composition of vegetation fire particles and the important photochemistry occurring in the tropics are likely to favor the buildup of polar oxygenated organic functions [*Kotzick and Niessner*, 1998]. Also, the presence of high amounts of alkaline metals (Na^+, K^+) enhances the water solubility of the weak organic acids [*Saxena and Hildemann*, 1996]. This result is important since hydrophilic compounds are expected to increase aerosols ability to act as cloud condensation nuclei (CCN). From 80 to 100% of biomass burning submicron particles were found to possibly act as CCN [*Rodgers et al.*, 1991] and, furthermore, capping clouds are frequently observed above smoke plumes [*Andreae*, 1993]. The CCN release from African savannas fires only has been estimated to be on a global scale, comparable to other natural and anthropogenic sources [*Dinh et al.*, 1994]. If the CCN behavior of biomass fire particles can be attributed to water-soluble inorganic substances (such as sulfate, nitrate, potassium, sodium, ammonium), our results suggest that the large amount of WSOC in the particulate phase may possibly also be responsible for this CCN behavior.

For the particulate PAHs speciation, 13 samples representing the FBL, the SBL, and the HL were analyzed. In Table 3, average concentrations for each layer are presented. Particulate PAHs concentrations were found to be much more variable (600 to 15,000 pg m^{-3}) than the total carbon content of the aerosols (OM from 14 to 130 $\mu g\ m^{-3}$). This result points out emission factors variability and perhaps the PAHs' sensitivity to photochemical oxidation. Phenanthrene was always, by far, the most abundant PAH, representing on average 40% of the total particulate PAHs mass. According to the chemical reactivity of phenanthrene, its abundance confirms the major influence of nearby sources. Surprisingly, notable amounts of retene were also present in some samples (Table 3). Retene is attributed to the degradation of abietic acid and is usually used as a tracer of conifer burning [*Ramdahl*, 1983]. However, more recent works have shown that some deciduous species in temperate regions [*König et al.*, 1995] or in tropical bush [*Guenther et al.*, 1996] could be also terpene emitters. The presence of retene in some of our samples could be explained by the burning of such species. A careful look at air mass back trajectories could not give any indication on a particular source region, and the emission of retene appears as the fingerprint of individual fires more than that of a representative regional ecosystem.

The sum average, from which phenanthrene, retene, anthracene, and benzo(a)anthracene were excluded, (ΣPAH = fluoranthene + pyrene + chrysene + benzo(b)fluoranthene + benzo(k)fluoranthene + benzo(a)pyrene + benzo(e)pyrene + benzo(ghi)perylene + coronene) measured here (700 ± 380 pg m^{-3}, n = 13), is lower compared to what was measured for the same nine PAHs at the savanna site of Lamto at ground level (2180 ± 110 pg m^{-3}, n = 3) [*Masclet et al.*, 1995], except for the exceptionally high value (ΣPAH = 10,540 pg m^{-3}) obtained for the HL sample 51/03. In Figure 7 we present the mean profiles of individual PAH abundance for the SBL, HL, and FBL samples. These profiles are globally very similar, the most abundant PAH being always fluoranthene, with also notable concentrations of chrysene, benzo(b)fluoranthene, and pyrene. Some differences are observed, among which the most striking point is the relatively low content of pyrene and the high content of benzo(b)fluoranthene in airborne EXPRESSO aerosols compared to Lamto aerosols. This discrepancy could reflect differences in source emissions. Thus our data confirm that biomass burning is a source of numerous PAHs as found in urban plumes. They also show the difficulty in using a single PAH as a tracer of a given type of combustion. On the contrary, the use of some PAHs ratios may help to identify the sources. For instance, in our samples the ratio benzo(ghi)perylene/pyrene is lower (0.31 ± 0.4, n = 11) than found in urban plume (2.5) [*Masclet et al.*, 1995].

On average, ΣPAH represents 0.0021 ± 0.0011% (n = 6) of the particulate organic carbon. An interesting feature of the data is the mean ΣPAH/BC ratio value obtained here (0.013 ± 0.012%, n = 6), which is 1 order of magnitude less than at Lamto ground level (0.12 ± 0.04%, n = 3). This could be attributed to a decay of PAHs by oxidation processes when transported to higher altitudes. It has been shown in chamber experiments that the destruction of PAHs is enhanced when the species are adsorbed on BC aerosols, the major effect of which is probably to focus light radiations toward the particles. For nine unbranched major PAHs submitted to moderate humidity, temperature, and light conditions, a lifetime of the order of 1 hour had been evaluated [*Kamens et al.*, 1988]. Although the photochemical destruction of PAHs could be particularly intense in the conditions of the EXPRESSO experiment (with high BC concentrations and intense sunlight radiations), the lifetime of PAHs is probably higher than expected from chamber experiments since significant amounts of these PAHs were still encountered in the HL several days after their emissions.

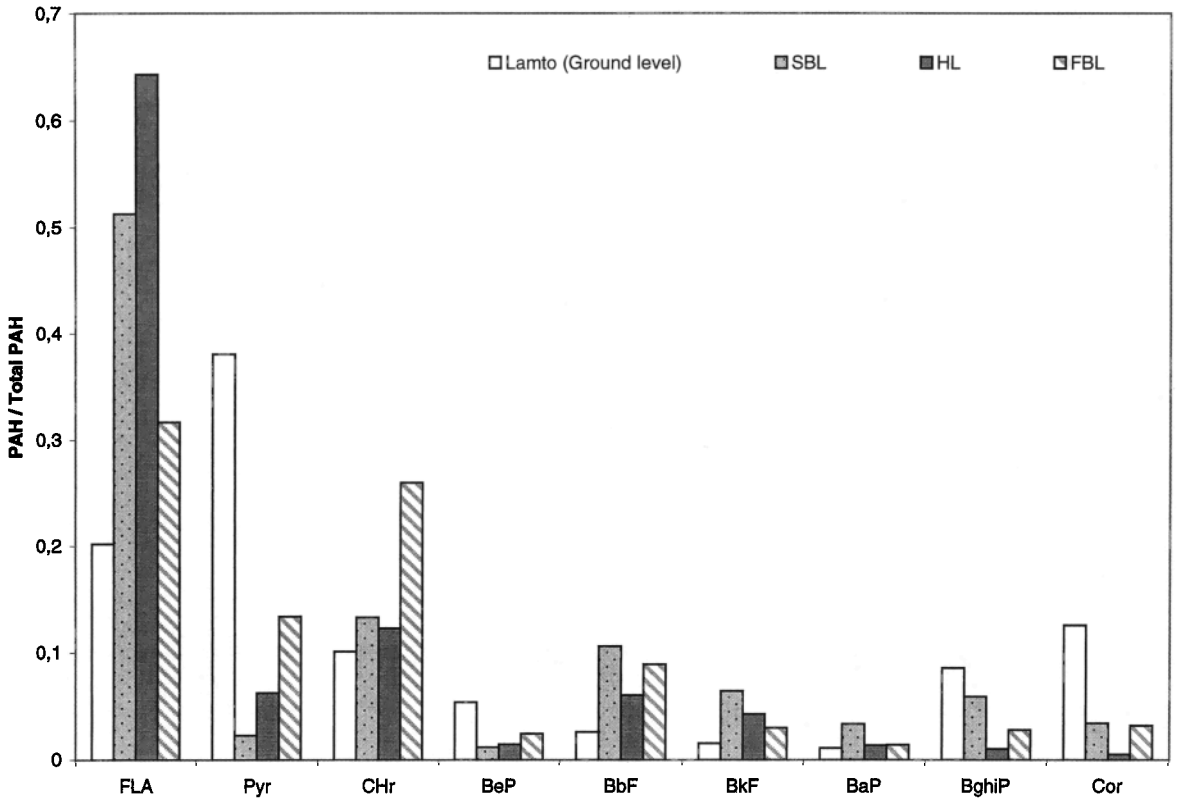

Figure 7. Average PAHs distribution obtained in each layer. Phenanthrene, retene, anthracene, and benzo(a)anthracene are excluded here; each PAH is normalized to the sum of the nine PAHs presented.

An interesting example is the exceptionally high ΣPAH/BC ratio (0.13) obtained for the 51/03 HL sample. Moreover, the mean value of the ($1\text{-}NO_x/NO_y$) ratio used as an indicator of the photochemical age of the air mass (T. Marion et al., unpublished manuscript, 1999) was significantly lower (0.4) for this sample than the HL average values (0.6 ± 0.1, $n = 7$). These indicators both suggest the presence of younger than expected air in the HL and might be the sign of intrusion of fresh fire inputs in the upper layers. Indeed, some intense savanna fires have been reported to have injection height over 2500 m [*Stocks et al.*, 1996]. Our experimental data suggest that in conditions where biomass burning sources are similar, the PAHs photochemical decay, and more specifically the ΣPAH/BC ratio, could be used as an indicator of aerosol aging. If so, the gradual increase of ratio values observed from ground level to HL could reflect an increase of the aerosol age residing in each atmospheric layer. Also, it may be noticed that the relative abundance of the major PAH (fluoranthene) seems to increase with the aerosol age. This is compatible with what is known on its reactivity in photochemical processes [*Masclet et al.*, 1986]. Fluoranthene abundance in the PAHs distribution could be also proposed to serve as an indicator of the age of biomass burning aerosols.

5.4. Ion Species

Concentrations of particulate ions were measured by ion chromatography and are reported in Table 4. For data interpretation, mean concentrations were normalized relative to BC (used as an inert biomass burning tracer): $X_{BC} = [X]/[BC]$. These normalized concentrations are represented

Table 4. Mean Chemical Composition of Aerosols

		Acetate	Formate	Chloride	Nitrate	Sulfate	Oxalate	Sodium	Ammonium	Potassium	Magnesium	Calcium
Savanna (2)	Mean	0.01	0.02	0.02	0.04	0.93	0.14	0.03	0.10	0.24	0.02	0.10
(ground level)	s.d.	0.00	0.00	0.01	0.02	0.39	0.05	0.01	0.03	0.06	0.01	0.02
SBL (8)	Mean	0.61	0.48	0.20	0.58	4.35	0.82	0.85	0.41	0.83	0.07	0.35
	s.d.	0.12	0.23	0.16	0.19	1.73	0.18	0.29	0.16	0.27	0.05	0.11
FBL (6)	Mean	0.44	0.37	0.24	0.34	1.97	0.65	0.71	0.25	0.52	0.05	0.21
	s.d.	0.12	0.13	0.18	0.11	1.22	0.30	0.27	0.15	0.36	0.02	0.11
HL (7)	Mean	0.85	0.52	0.39	0.90	4.58	1.17	1.07	0.39	1.14	0.10	0.49
	s.d.	0.53	0.15	0.47	0.59	3.32	0.50	0.45	0.28	0.82	0.09	0.43
Lamto (10)	Mean	...	...	1.1	3.5	2.56	0.62	0.8	0.12	0.9	0.3	1.9
	s.d.	...	...	0.16	0.5	0.38	0.1	0.1	0.02	0.1	0.05	0.22

Concentrations in $\mu g\ m^{-3}$. Here n is number of samples; s.d., standard deviation. Lamto data from *Yoboué* [1991] (average of January 1988 and January 1989 concentrations) and *Cachier et al.* [1991].

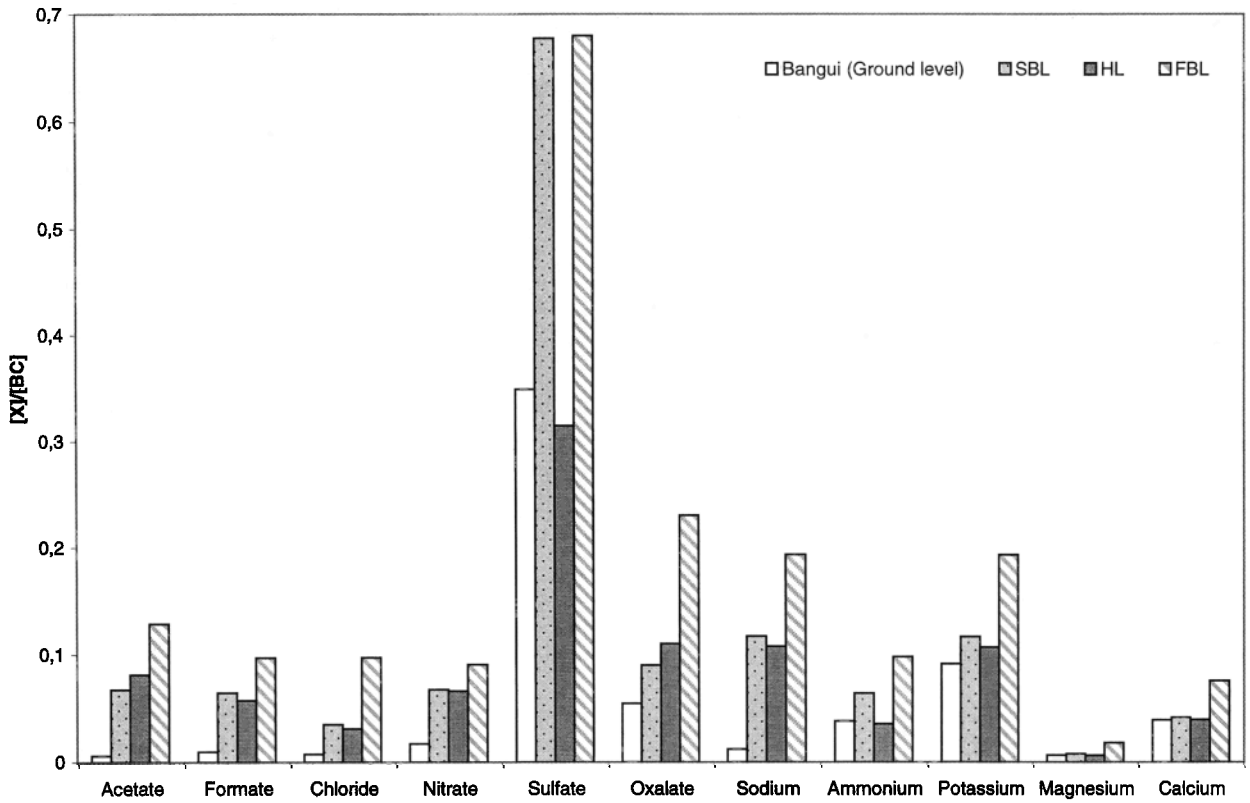

Figure 8. Ion mass concentrations ($X_{BC} = [X]/[BC]$) normalized to black carbon (BC) mass concentration.

on Figure 8. On average, the normalized concentrations measured during EXPRESSO are lower than expected by comparison with airborne concentrations obtained during the SAFARI experiment [*Andreae et al.*, 1998] and Smoke, Clouds, and Radiation-Brazil (SCAR-B) experiment [*Reid et al.*, 1998] or ground data obtained in the savanna site of Lamto [*Cachier et al.*, 1991]. This may be due to the exceptionally important levels of particulate carbon encountered during EXPRESSO and/or the effect of preferential washout of ion aerosols by some residual rains encountered by the time of the experiment.

Most of the compounds analyzed may have different sources: biogenic (forest), marine (oceanic inputs in the monsoon flux), and savanna fires [*Gaudichet et al.*, 1995; *Maenhaut et al.*, 1996]. Some of them are considered as biomass burning tracers [*Andreae*, 1983; *Baudet et al.*, 1990; *Legrand et al.*, 1992].

Comparison of K and S concentrations obtained by XRF and IC measurements shows that these species are mainly soluble (70 and 84%, respectively). This is an additional indicator of the predominant biomass burning origin for these two elements appearing in the particulate phase mostly as cristalline condensates. The mean insoluble potassium concentration (K measured by XRF − K measured by IC) was found to be of 0.55 ± 0.47 $\mu g\ m^{-3}$ ($n = 20$). Considering the mean of the K/Al ratio in dusts (0.25), from this value dust concentration is evaluated to be 31 ± 27 $\mu g\ m^{-3}$ ($n = 20$), which is in good agreement with what was found from Al data (section 5.2).

Consequently, sulfate is likely to be mainly originating from the secondary conversion of SO_2 emitted by fires. This species is in our data set the most abundant compound, with concentrations of the same order as black carbon. Average $SO_{4\ BC}^{=}$ (0.53 ± 0.4, $n = 15$) is of the same order as that obtained in the background of Lamto (0.5 ± 0.2) [*Yoboué*, 1991; *Cachier et al.*, 1991]. For the ground and Harmattan samples, average normalized $SO_4^=$ ($SO_{4\ BC}^{=}$) is lower (0.31 ± 0.02, $n = 5$) than for the BL samples where unexpected higher values are observed (0.7 ± 0.8, $n = 12$). A possible explanation for these high values encountered in the BL could be the resuspension during fires of biogenic reduced sulfur species deposited on the vegetation, originating from the wet forest bogs.

Primary compounds (K^+, Ca^{++}, and Mg^{++}) display very constant concentrations except in the FBL. Recalling that these concentrations are normalized to BC, this feature could confirm that the ions primarily originate from fires, as a constituent of the vegetation fuel or by resuspension of dusts previously deposited on the leaves. FBL-normalized concentrations of K^+, Ca^{++}, and Mg^{++} are the highest of the data set which suggests that the forest is an additional source for these elements. Na^+ concentrations are quite constant in the different atmospheric layers except at ground level. This result could also indicate that marine air trapped in the monsoon layer may escape the FBL and exchange with other layers.

The presence of organic (formate, acetate, and oxalate) species and nitrate in the particulate phase is due to the secondary formation by photochemical oxidation of gases and subsequent neutralization by alkaline species. The amount of ion aerosols is thus due to the combination of a flux of gaseous precursors, the oxidation kinetics (which is probably the limiting step), and the amount of alkaline species (Ca^{++}, Na^+, and K^+) in the aerosol phase. For all considered species there is an increase of concentration from the ground to the HL, which could point out the importance of the limiting photooxidation step. However, for some of the species, SBL and HL concentrations are quite similar which could indicate that the secondary formation and subsequent neutralization by alkaline ions is rapidly com-

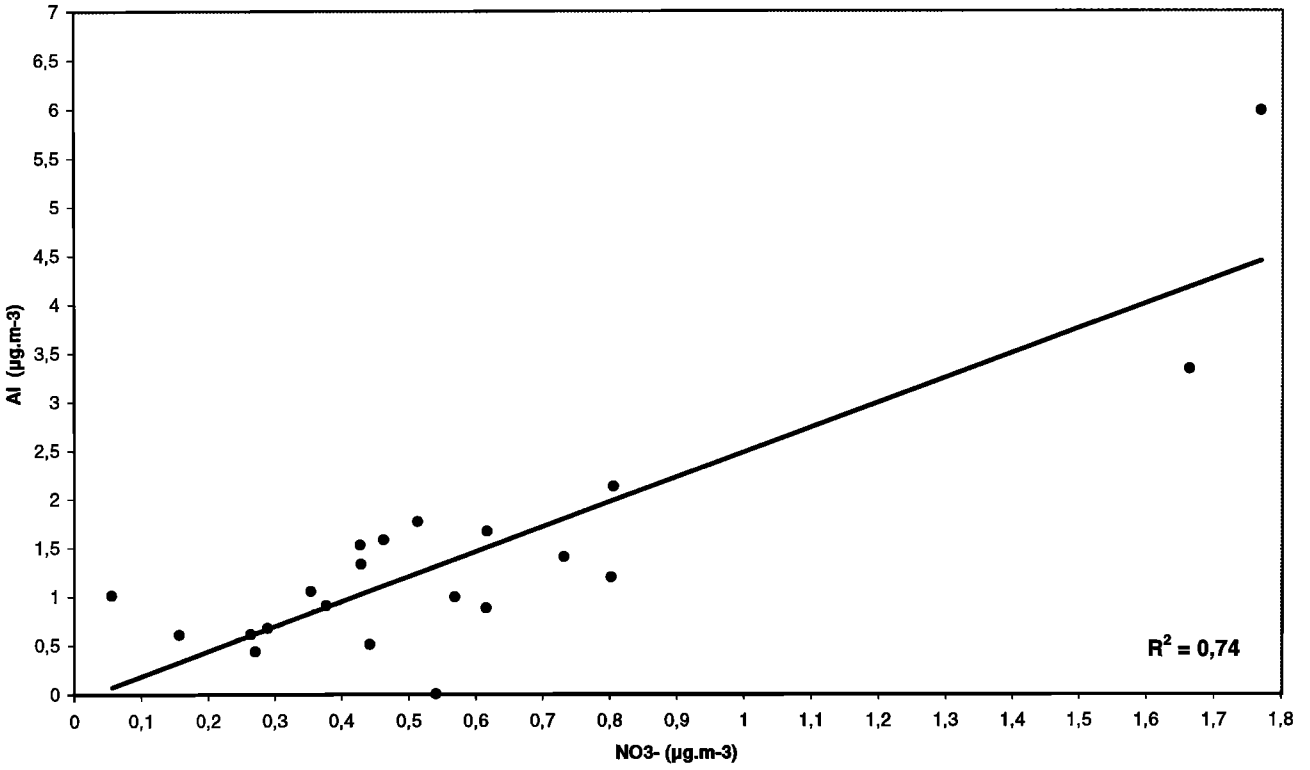

Figure 9. Correlation between particulate nitrate and Al concentrations. Data from all layers.

pleted. Only for acetate, and especially oxalate, the abundance still increases in the HL, which points to formation rates which could be significantly slower than for formate and nitrate. However, alkaline species show a fair covariation with formate and acetate. As formate and acetate amounts found in the aerosol phase are remarkable, considering their vapor pressures at the ambient temperature encountered during the EXPRESSO experiment, the second factor (limitation by the amount of alkaline ions) might be important. An interesting feature is also that formate, acetate, and oxalate are more abundant in the FBL, confirming that the forest is a source of gaseous organic acids [*Lefeivre*, 1993; *Jacob and Wofsy*, 1988; *Graedel et al.*, 1986]. However, this source appears to be particularly active for oxalate aerosols for which a biogenic origin or the emission of precursors by vegetation cannot be excluded. An explanation could be related to the presence of oxalate in some plant tissues which could produce primary biogenic particles. The remarkable amounts of organic acids found here may strongly contribute to the aerosol phase ionic balance. However, because some important ionic species such as carbonate or H^+ were not measured, it has not been possible to check this hypothesis.

Nitrogen-containing ions are primarily NO_3^- and NH_4^+ with similar concentrations. NH_4^+ is, however, more abundant than NO_3^- at ground level which could be due to the secondary origin of nitrate. The presence of relatively high concentrations of the reduced species NH_4^+ could be an indicator of intense fires accompanied by the formation of oxygen-depleted air pockets [*Cofer et al.*, 1989; *Cachier et al.*, 1995]. The presence of NO_3^- in the particulate phase is likely due to the neutralization and attachment of gaseous nitric acid to soil-derived particles [*Cachier et al.*, 1991; *Dentener et al.*, 1996]. Consistent results obtained at Lamto by impactor measurements and showing similar size distribution of NO_3^- and Ca^{++} [*Cachier et al.*, 1991] confirm this hypothesis. Here we also show a satisfactory correlation between Al and NO_3^- (Figure 9) underlying the role of dusts in the incorporation of NO_3^- in the particulate phase. Consequently, low NO_3^- concentrations are expected in the aerosol phase due to the poor concentration of dust during EXPRESSO. In Lamto, where dust concentrations were more abundant (from 40 to 60 $\mu g\ m^{-3}$), particulate $NO_{3\,BC}^-$ (0.8) is 1 order of magnitude higher than the EXPRESSO average (0.07). However, in both experiments, carbonate abundance could have been one of the limiting agents for the incorporation of NO_3^- in the aerosols since the NO_3^-/Ca^{++} ratio is comparable (1.5 and 2, respectively). These results confirm the determinant role of alkaline soil-derived particles for the neutralization of gaseous nitric acid. However, another hypothesis could be the trapping of nitrates (and other gases such NH_3) into the clay matrix [*Deer et al.*, 1966; *Martin et al.*, 1986]. Finally, it may be noted that due to the low dust atmospheric concentration during the EXPRESSO experiment, most nitrate originating from the numerous savanna fires was in the gaseous form. This is in good agreement with the gaseous HNO_3 concentrations calculated from NO_z ($NO_z = NO_y - NO_x$) measurements (T. Marion et al., unpublished manuscript, 1999), showing 1 order of magnitude difference between gaseous HNO_3 and particulate NO_3^- (4.6 and 0.6 $\mu g\ m^{-3}$, respectively). Therefore, in the conditions of the EXPRESSO campaign, the partition between the gaseous and the particulate phase is in favor of the gaseous phase. The atmospheric lifetime of nitrate and probably other species such as NH_3 or light organic acids differs considerably from what is expected if these species were primarily attached to dust aerosols. Indeed, most of these gases are likely to undergo efficient dry deposition, whereas particulate NO_3^-, NH_4^+, or formate will be pri-

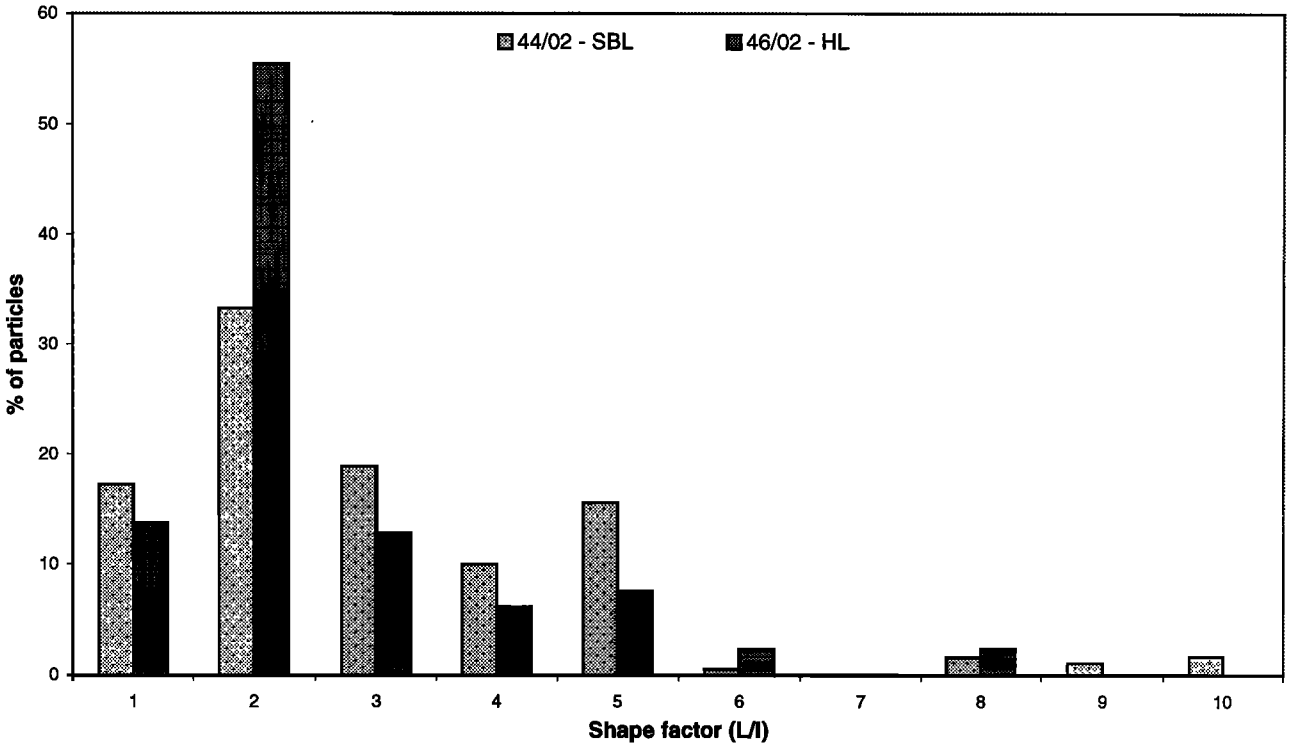

Figure 10. Shape factor (L/l) distribution for a savanna boundary layer (44/02) and a Harmattan layer (46/02) sample. Only particles with $L > 0.5$ μm are taken into account (the number of particles studied is 261 and 242, respectively). SBL sample is considered as a "young" aerosol (34% of particles with $L/1 < 2.5$). HL sample is an "old" aerosol (78% of particles with $L/1 < 2.5$).

marily scavenged from the atmospheric reservoir by rain out processes [*Lacaux et al.*, 1991]. We also suggest that at the beginning of the dry season, in the absence of dust, the translocation of nitrates by fires could be confined in the region. Contrarily, further in the season, when the atmosphere is heavily impregnated by dust, wet scavenging of nitrogen-containing species as particulates could cause a notable loss of nutrients.

6. Aging Indicators

The variable distance to sources during the different sample collections has also allowed to gain some indications on the physicochemical aging of particles. Microscopy observations were conducted on two representative samples: a savanna sample (44/02) assessed to contain "young" aerosols and a Harmattan sample (46/02) with older particles. We tried to see any change in the morphology of microsoot particles which could be associated with aging processes. Investigations relied both on size and shape of the particles. For the size study we chose a threshold of 0.5 μm for the highest dimension (L) to differentiate small and coarse microsoots, and with this cut, "young" aerosols appear characteristically smaller than "old" ones with 31 and 23%, respectively, of particles below 0.5 μm. We defined also a shape factor (L/l) corresponding to the ratio of the highest to the smallest dimension, determined on coarse microsoots ($L > 0.5$ μm) only. Figure 10 shows that aging appears in the shape factor as a tendency to more spherical aggregates.

The ratio particle number density/black carbon mass concentration (CN/BC) is expected to decrease with particle aging due to aggregation and coagulation processes occurring during the transport. Indeed, this ratio is found to be higher in the boundary layer than in the HL. In the FBL this ratio is very variable and might be enhanced by the presence of fresh biogenic particles.

In Table 5 we recall the different chemical indicators which can be used for the bulk composition of combustion aerosols. Particle aging may be related to the formation of secondary species and is visualized by the evolution of their abundance relative to inert biomass burning constituents such as K or BC. For sulfate the S/BC and S/K ratios were previously found to increase rapidly from the fresh plumes to the savanna background atmosphere at ground level [*Cachier et al.*, 1995; *Gaudichet et al.*, 1995]. In Bangui the S/K ratio is similar to the Lamto background value, and only a slight increase is observed for the airborne particles in the HL. This result indicates that the major transformations affecting the S content of the aerosols occur rapidly close to the fires. However, oxalate which is found in notable concentration in biomass burning aerosols appears to be formed less rapidly, and its abundance increases gradually in the different atmospheric layers.

The aging of the carbonaceous content of aerosols has been related to a partial loss of their organic content by photooxidation processes [*Liousse et al.*, 1995]. This loss shows up as an increase of the BC/TC ratio during atmospheric transport. Although the BC/TC ratio may be utilized as an indicator of burning processes [*Cachier et al.*, 1996], it has been found to reflect the particle age with values ranging from 10 $\pm$ 4% in the plume to 26 $\pm$ 5% in the background atmosphere of savanna fires [*Cachier et al.*, 1995; *Andreae et al.*, 1998; *Reid et al.*, 1998].

Table 5. Biomass Burning Aging Indicators

	n	BC/TC, %	CN/BC Ratio	1 − NO_x/NO_y Ratio	WSOC/OC, %	K/BC Ratio	S/BC Ratio	S/K Ratio	Oxalate/BC Ratio	ΣPAH/BC, %
Savanna ground level	2	20 ± 8	···	···	27 ± 5	0.2	0.16	0.03	0.05 ± 0.01	···
SBL mean	4	19 ± 2	414 ± 140	0.11 ± 0.01	46 ± 23	0.16 ± 0.05	0.35 ± 0.3	1.3 ± 0.35	0.09 ± 0.02	0.008 ± 0.004
	45/01	22	65	0.1	30	0.18	0.26	1.42	0.09	0.14
FBL mean	4	21 ± 9	675 ± 460	0.2 ± 0.2	51 ± 31	0.17 ± 0.25	0.15 ± 0.02	1.1 ± 0.25	0.15 ± 0.09	0.035
	46/01	8	178	0	12	0.63	0.92	1.45	0.37	···
HL mean	3	23 ± 6	24 ± 4	0.6 ± 0.1	85 ± 18	0.13 ± 0.02	0.24 ± 0.08	1.1 ± 0.15	0.11 ± 0.04	0.005
	5203	16	345	0.7	···	···	···	···	0.10	···
Lamto (plume)	···	12 ± 3	···	···	···	0.64 ± 0.28	···	0.06	···	···
Lamto (background)	···	19.8 ± 4	···	···	···	0.23 ± 0.03	···	0.4–0.7	0.15 ± 0.02	0.12 ± 0.04

Values given are means and standard deviations. Here *n* is number of samples. CN/BC in $cm^{-3}/\mu g\ m^{-3}$. Lamto data from *Yoboué* [1991], *Cachier et al.* [1995], *Gaudichet et al.* [1995], and *Masclet et al.* [1995].

The BC/TC ratio found here at ground level is on average of 20 ± 6% (n = 2). A slight increase of this ratio is indeed observed here in the SBL and Harmattan samples, and a comparison of the three BC/TC values (FBL, SBL, and HL) suggests that the main transformations undergone by organic aerosols also take place rapidly close to the fires. However, any statement on aging through the BC/TC ratio remains questionable due to the variability of this ratio inside a given atmospheric layer. Further slow aging of particulate and gaseous organic species is expected to occur off source regions. In the FBL the expected disappearance of OC is not as marked as in the Harmattan layer which could be due to additional inputs of biogenic aerosols. This effect is particularly visible for sample 46/01 which is the less affected by savanna fires. For this sample the BC/TC value (8%) is exceptionally low. The important transformations due to photochemical aging affect also the WSOC content. Figure 11 shows a satisfactory positive correlation (r^2 = 0.83) between WSOC/OC and the photochemical age indicator (1 − NO_x/NO_y) (T. Marion et al., unpublished manuscript, 1999), confirming the creation of polar functionalities and thus the increase of WSOC content of aerosol by photochemical aging. A positive covariation between WSOC/OC and BC/TC (r^2 = 0.51) is also observed recalling that the photochemical attacks of carbonaceous particles favors simultaneously the formation of water-soluble species and the partial degradation and consecutive loss of particulate OC.

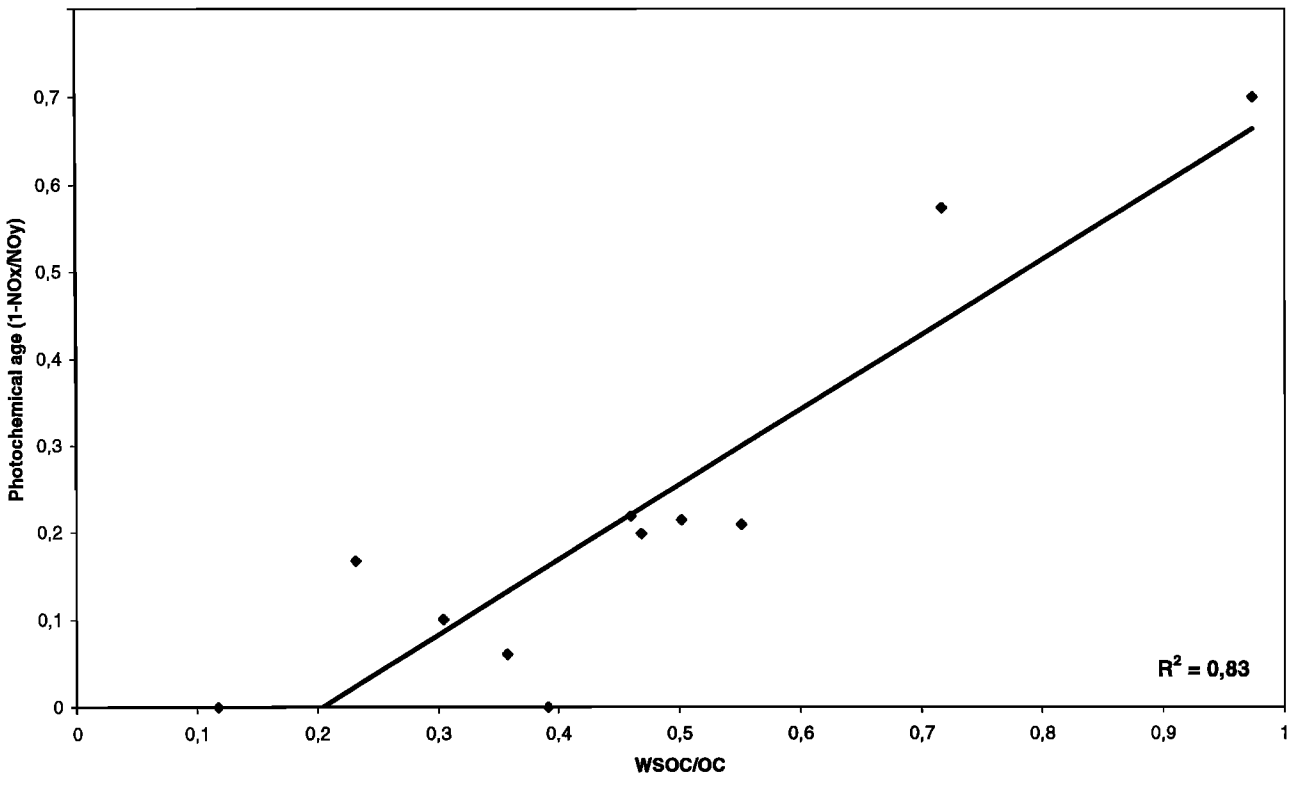

Figure 11. Correlation between the photochemical age (1 − NO_x/NO_y) as defined by T. Marion et al. (unpublished manuscript, 1999) and the water solubility of organic particles (defined by WSOC/OC).

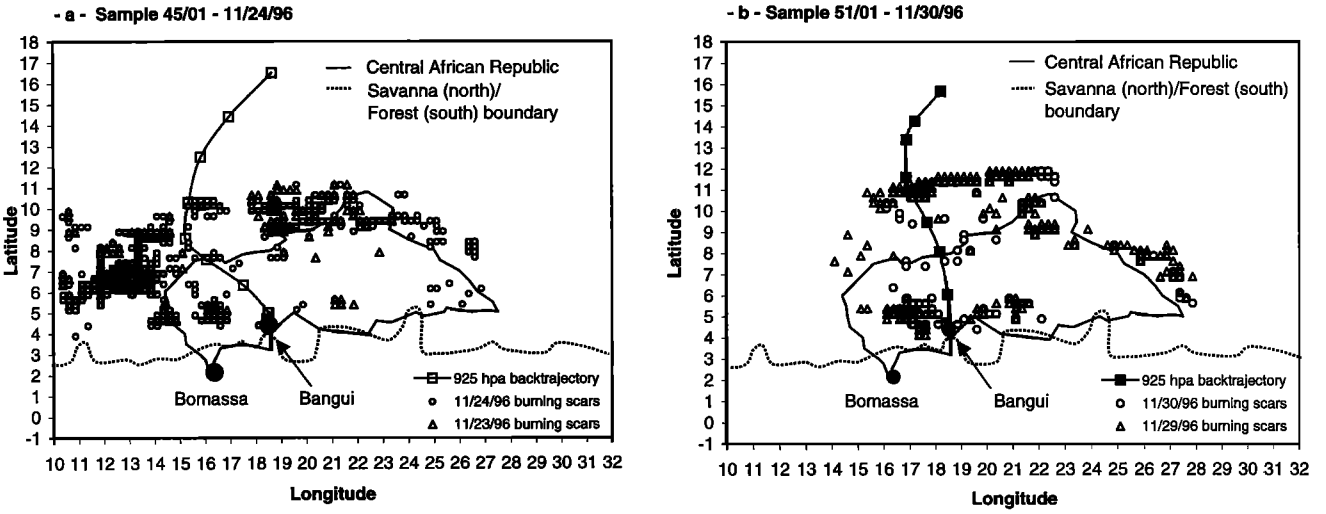

Figure 12. Distribution of burning scars detected the day (open circles) and the day before (open triangles) (a) sample 45/01 (low concentrations) and (b) sample 51/01 (high concentrations). Remote sensing data from *Grégoire et al.* [this issue] and *Pereira et al.* [this issue]. Only cells (0.25° × 0.25°) for which the burning scars area is larger than 50 km^2 are presented. Four-day back trajectory calculated from ECMWF data (one point every 12 hours).

In conclusion, for all layers the chemical aging indicators and the morphological criteria point to a somewhat "old" combustion aerosol either in the BL or in the HL with, most of the time, some additional aging marks for the HL aerosols.

Owing to concordant informations of aging indicators, some comments may be proposed on "odd" samples. If, on average, HL samples display the characteristics of aged particles (Table 5), the Harmattan sample 52/03 seems to be younger (low BC/TC and high CN/BC ratios). This could be due to incursions of fresh fire aerosols in the HL as also previously hypothesized for the Harmattan sample 51/03 (section 5.3). In the SBL, aging indicators confirm the presence of less old aerosols than in the HL. For one sample (45/01), however, an unexpectedly low CN/BC ratio value and an exceptionally low particle number concentration (415 cm^{-3}) suggest that the influence of vicinal savanna fires was very low and that particles were older than expected. Indeed, from satellite data (Figure 12a) it may be seen that burning scars are scarce along the air mass track related to flight 45/01. On the contrary, for other SBL samples, the air mass track and sampling locations were often very closed to burning areas as seen in Figure 12b for flight 51/01.

7. Conclusion

High airborne concentrations of pyrogenic particles were found in each atmospheric layer, and over the forest, also, pyrogenic particles were abundant. Despite some physicochemical evolution of particles, the fire signature could be identified and was ubiquitous. Moreover, it has been shown that a notable fraction of the other inorganic or crustal aerosol particles could have been formed or entrained in the atmosphere by fires. These results underline the overwhelming regional influence of savanna fires on the troposphere over central Africa. It has been shown that biomass burning aerosols emitted at northern latitudes are transported in the Harmattan flux, whereas those found in the BL originated mostly from more local burns. However, our work suggests exchanges between the different atmospheric layers as well as through the ITCZ. These vertical and horizontal exchanges might be due to atmospheric subsidence or turbulence (C. Delon et al., unpublished manuscript, 1999) at the edge of the forest. Intense savanna fires may also be responsible for vertical exchanges. It must be recalled that the experiment took place at the very beginning of the dry season which suggests that for the following months still higher concentrations could have been expected, especially in the BL due to the southward shift of the main fire zones. The onset of the dry season was observed along the experiment leading to, although lower than expected, increasing soil-derived particle concentrations. The overall low dust concentrations favored the gas/particle partition of species such as nitrate or light organic acids toward the gaseous phase which could result in important acidic dry deposition.

Finally, the work presented here may be considered as a preliminary step for further modeling studies of the atmospheric impact of tropical biomass burning aerosols. From the use of different aging indicators such as the WSOC/OC ratio or the shape factor of particles, it was assessed that aging of biomass burning particles significantly affects their inorganic and organic content, as well as their morphology. Aging processes are also expected to increase the heterogeneity of particles.

It appears thus mandatory to accurately take into account the physical and chemical properties of particles to evaluate their optical and radiative properties as well as their ability to act as a CCN agent. An important parameter could be the water solubility of biomass burning aerosols which appears to be significant (on average, nearly half of the organic aerosols are water soluble), especially in the Harmattan layer where they have undergone photochemical transformations.

Acknowledgments. This experimental work was supported by the Centre National de la Recherche Scientifique in the frame of a specific action of the PNCA. The authors wish to thank the scientific and technical crew as well as the pilots of the research aircraft. We also thank Laurent Gomes and Michel Maillé from the LISA for their

contribution during the preparation of the experiment. We are indebted to Désiré Malibangar, Louis Matos, and Dominique Serça for their help in Bangui and Bomassa. Finally, we would like to gratefully acknowledge the determinant and motivating contribution of Bernard Cros for the organization of the experiment in spite of adverse conditions.

References

Anderson, B. E., W. B. Grant, G. L. Gregory, E. V. Browell, J. E. Collins Jr., G. W. Sachse, D. R. Bagwell, C. H. Hudgins, D. R. Blake, and N. J. Blake, Aerosols from biomass burning over the tropical South Atlantic region: Distribution and impacts, *J. Geophys. Res.*, *101*, 24,117–24,137, 1996.

Andreae, M. O., Soot carbon and excess fine potassium: Long-range transport of combustion-derived aerosols, *Science*, *220*, 1148–1151, 1983.

Andreae, M. O., The influence of tropical biomass burning on climate and the atmospheric environment, in *Biochemistry of Global Change: Radiative Active Traces Gases*, edited by R. S. Oremland, pp. 113–150, Chapmann and Hall, New York, 1993.

Andreae, M. O., et al., Biomass burning in the global environment: First results from the IGAC/BIBEX field campaign STARE/TRACE-A/SAFARI-92, in *Global Atmospheric-Biospheric Chemistry*, edited by R. G. Prinn, pp. 83–101, Plenum, New York, 1994.

Andreae, M. O., et al., Airborne studies of aerosol emissions from savanna fires in southern Africa, 2, Aerosol chemical composition, *J. Geophys. Res.*, *103*, 32,119–32,128, 1998.

Artaxo, P., E. T. Fernandes, J. V. Martins, M. A. Yamasoe, P. V. Hobbs, W. Maenhaut, K. M. Longo, and A. Castanho, Large-scale aerosol source apportionment in Amazonia, *J. Geophys. Res.*, *103*, 31,837–31,847, 1998.

Baudet, J. G. R., J. P. Lacaux, J. J. Bertrand, and F. Desalmand, Presence of an atmospheric oxalate source in the intertropical zone: Its potential action in the atmosphere, *Atmos. Res.*, *25*, 465–477, 1990.

Bowen, H. J. M., *Trace Elements in Biochemistry*, Academic, San Diego, Calif., 1966.

Brémond, M. P., Contribution à l'étude géochimique du carbone-suie dans l'atmosphère: Aspects méthodologiques et géochimiques (in French), Ph.D. dissertation, Univ. Paris VII, Paris, 1989.

Cachier, H., Biomass burning sources, in *Encyclopedia of the Earth Science System*, edited by N. Nierenberg, pp. 377–385, Academic, San Diego, Calif., 1992.

Cachier, H., P. Buat-Ménard, M. Fontugne, and R. Chesselet, Long-range transport of continentally-derived particulate carbon in the marine atmosphere: Evidence from stable carbon isotope studies, *Tellus, Ser. B*, *38*, 161–177, 1986.

Cachier, H., M. P. Brémond, and P. Buat-Ménard, Determination of atmospheric soot carbon with a simple thermal method, *Tellus, Ser. B.*, *41*, 379–390, 1989.

Cachier, H., J. Ducret, M.-P. Brémond, V. Yoboué, J. L. Lacaux, A. Gaudichet, and J. Baudet, Biomass burning aerosols in a savanna region of the Ivory Coast, in *Global Biomass Burning: Atmospheric, Climatic and Biospheric Implications*, edited by J. S. Levine, pp. 174–180, MIT Press, Cambridge, Mass., 1991.

Cachier, H., C. Liousse, and P. Buat-Ménard, Particulate content of savanna fire emissions, *J. Atmos. Chem.*, *22*, 123–128, 1995.

Cachier, H., C. Liousse, M. H. Pertuisot, A. Gaudichet, F. Echalar, and J. P. Lacaux, African fire particulate emissions and atmospheric influence, in *Biomass Burning and Global Change*, edited by J. S. Levine, pp. 428–440, MIT Press, Cambridge, Mass., 1996.

Cadle, S. H., and P. J. Groblicki, An evaluation of methods for the determination of organic and elemental carbon in particulate samples, in *Particulate Carbon-Atmospheric Life Cycle*, edited by G. T. Wolff and R. L. Klimisch, pp. 89–109, Plenum, New York, 1982.

Cautenet, S., D. Poulet, C. Delon, R. A. Delmas, J. M. Gregoire, M. Pereira, S. Cherchali, O. Amram, and G. Flouzat, Simulation of carbon monoxide redistribution over central Africa during biomass burning events (EXPRESSO experiment), *J. Geophys. Res.*, this issue.

Chiapello, I., G. Bergametti, L. Gomes, B. Chatenet, F. Dulac, J. Pimenta, and E. Santos Suares, An additional low-layer transport of Sahelian and Saharian dust over the northeastern tropical Atlantic, *Geophys. Res. Lett.*, *22*, 3191–3194, 1995.

Clairac, B., R. Delmas, B. Cros, H. Cachier, P. Buat-Ménard, and J. Servant, Formation and chemical composition of atmospheric aerosols in an equatorial forest area, *J. Atmos. Chem.*, *6*, 301–322, 1988.

Cofer, W. R., III, J. S. Levine, D. I. Sebacher, E. L. Winstead, P. J. Riggan, B. J. Stocks, J. A. Brass, V. G. Ambrosia, and P. J. Boston, Trace gas emissions from chaparral and boreal forest fires, *J. Geophys. Res.*, *94*, 2255–2259, 1989.

Countess, R. J., S. H. Cadle, P. J. Groblicki, and G. T. Wolff, Chemical analysis of size-segregated samples of Denver's ambient particulate, *J. Air Pollut. Control Assoc.*, 247–252, 1981.

Crutzen, P., and M. O. Andreae, Biomass burning in the tropics: Impact on atmospheric chemistry and biogeochemical cycles, *Science*, *250*, 1669–1678, 1990.

Deer, W. A., R. A. Howie, and J. Zussman, *Rock-Forming Minerals*, Copp, Clark, Mississauga, Ont., 1966.

Dentener, F. J., G. R. Carmichael, Y. Zhang, J. Lelieveld, and P. J. Crutzen, Role of mineral aerosol as a reactive surface in the global troposphere, *J. Geophys. Res.*, *101*, 22,869–22,889, 1996.

Dinh, P. V., J. P. Lacaux, and R. Serpolay, Cloud-active particles from African savanna combustion experiments, *Atmos. Res.*, *31*, 41–58, 1994.

Echalar, F., A. Gaudichet, H. Cachier, and P. Artaxo, Aerosol emissions by tropical forest and savanna biomass burning: Characteristic trace elements and fluxes, *Geophys. Res. Lett.*, *22*, 3039–3042, 1995.

Galy-Lacaux, C., and A. I. Modi, Precipitation chemistry in the Sahelian savanna of Niger, Africa, *J. Atmos. Chem.*, *30*, 319–343, 1998.

Gaudichet, A., J. R. Petit, R. Lefèvre, and C. Lorius, An investigation by analytical transmission electron microscopy of individual insoluble microparticles from Antartic (Dome C) ice core samples, *Tellus, Ser. B*, *38*, 250–261, 1986.

Gaudichet, A., F. Echalar, B. Chatenet, J. P. Quisefit, G. Malingre, H. Cachier, P. Buat-Ménard, P. Artaxo, and W. Maenhaut, Trace elements in tropical African savanna biomass burning aerosols, *J. Atmos. Chem.*, *22*, 19–39, 1995.

Graedel, T. E., D. T. Hawkins, and L. D. Claxton, *Atmospheric Chemical Compounds: Sources, Occurrence and Bioassay*, Academic, San Diego, Calif., 1986.

Grégoire, J.-M., S. Pinnock, E. Dwyer, and E. Janodet, Satellite monitoring of vegetation fires for EXPRESSO: Outline of activity and relative importance of the study area in the global picture of biomass burning, *J. Geophys. Res.*, this issue.

Grosjean, D., In situ organic aerosol formation during a smog episode: Estimated production and chemical functionality, *Atmos. Environ., Part A*, *26*, 953–963, 1992.

Guenther, A., L. Otter, P. Zimmerman, J. Greenberg, R. Scholes, and M. Scholes, Biogenic hydrocarbon emissions from southern African savannas, *J. Geophys. Res.*, *101*, 25,859–25,865, 1996.

Hao, W. M., D. E. Ward, G. Olbu, and S. P. Baker, Emissions of CO_2, CO, and hydrocarbons from fires in diverse African savanna ecosystems, *J. Geophys. Res.*, *101*, 23,577–23,584, 1996.

Hudson, J. G., J. Hallet, and F. Rogers, Field and laboratory measurements of cloud-forming properties of combustion aerosols, *J. Geophys. Res.*, *96*, 10,847–10,859, 1991.

Intergovernmental Panel on Climate Change (IPCC), Climate change 1994: Radiative forcing of climate change and an evaluation of the IPCC IS92 emission scenarios, New York, 1995.

Jacob, D. J., and S. C. Wofsy, Photochemistry of biogenic emissions over the Amazon forest, *J. Geophys. Res.*, *93*, 1477–1486, 1988.

Kamens, R. H., Z. Guo, J. N. Fulcher, and D. A. Bell, Influence of humidity, sunlight, and temperature on the daytime decay of polyaromatic hydrocarbons on the atmospheric soot particles, *Environ. Sci. Technol.*, *22*, 103–108, 1988.

König, G., M. Brunda, H. Puxbaum, C. Nicholas Hewitt, S. Craig Duckham, and J. Rudolph, Relative contribution of oxygenated hydrocarbons to the total biogenic VOC emissions of selected mid-European agricultural and natural plant species, *Atmos. Environ.*, *29*, 861–874, 1995.

Kotzick, R., and R. Niessner, The effect of aging processes on critical supersaturation ratios of ultrafine carbon aerosols, *Atmos. Environ.*, *33*, 2669–2677, 1998.

Lacaux, J. P., R. Delmas, B. Cros, B. Lefeivre, and M. O. Andreae, Influence of biomass burning emissions on precipitation chemistry in the equatorial forest of Africa, in *Global Biomass Burning: Atmospheric, Climatic and Biospheric Implications*, edited by J. S. Levine, pp. 167–173, MIT Press, Cambridge, Mass., 1991.

Lacaux, J. P., H. Cachier, and R. Delmas, Biomass burning in Africa: An overview of its impact on atmospheric chemistry, in *Fire in the*

Environment: The Ecological, Atmospheric and Climatic Importance of Vegetation Fires, edited by P. J. Crutzen and J. Goldammer, pp. 159–191, John Wiley, New York, 1993.

Lacaux, J. P., J. M. Brustet, R. Delmas, J. C. Menaut, L. Abbadie, B. Bonsang, H. Cachier, J. Baudet, M. O. Andreae, and G. Helas, Biomass burning in the tropical savannas of Ivory Coast: An overview of the field experiment Fire of Savannas (FOS/DECAFE 91), *J. Atmos. Chem.*, *22*, 195–216, 1995.

Lefeivre, B., Etude expérimentale et par modélisation des caractéristiques physiques et chimiques des précipitations collectées en forêt équatoriale africaine (in French), Ph.D. dissertation, Univ. Paul Sabatier, Toulouse, France, 1993.

Legrand, M., M. De Angelis, T. Staffelbach, A. Neftel, and B. Stauffer, Large perturbations of ammonium and organic acids content in the Summit-Greenland ice core: Fingerprint from forest fires?, *Geophys. Res. Lett.*, *19*, 473–475, 1992.

Levine, J. S., *Global Biomass Burning: Atmospheric, Climatic, and Biospheric Implications*, MIT Press, Cambridge, Mass., 1991.

Liousse, C., C. Devaux, F. Dulac, and H. Cachier, Aging of savanna biomass burning aerosols: Consequences on their optical properties, *J. Atmos. Chem.*, *22*, 1–17, 1995.

Maenhaut, W., I. Salma, J. Cafmeyer, H. J. Annegarn, and M. O. Andreae, Regional atmospheric aerosol composition and sources in the eastern Transvaal, South Africa, and impact of biomass burning, *J. Geophys. Res.*, *101*, 23,631–23,650, 1996.

Marenco, A., M. Macaigne, and S. Prieur, Meridional and vertical CO and CH_4 distributions in the background troposphere (70°N–60°S; 0/12 km altitude) from scientific aircraft measurements during the STRATOZ III experiment (June 1984), *Atmos. Environ.*, *23*, 185–200, 1989.

Martin, D., B. Ardouin, G. Bergametti, J. Carbonelle, R. Faivre-Pierret, G. Lambert, M. F. Le Cloarec, and G. Sennequier, Geochemistry of sulfur in Mount Etna plume, *J. Geophys. Res.*, *91*, 12,249–12,254, 1986.

Masclet, P., P. Pistikopoulos, and K. Nikolaou, Relative decay index and sources of polycyclic aromatic hydrocarbons, *Atmos. Environ.*, *20*, 439–446, 1986.

Masclet, P., H. Cachier, C. Liousse, and H. Wortham, Emissions of polycyclic aromatic hydrocarbons by savanna fires, *J. Atmos. Chem.*, *22*, 41–54, 1995.

Mason, B., *Principles of Geochemistry*, John Wiley, New York, 1966.

Moberg, J. P., I. E. Esu, and W. B. Malgwi, Characteristics and constituent composition of Harmattan dust falling in northern Nigeria, *Geoderma*, *48*, 73–81, 1991.

Novakov, T., and C. E. Corrigan, Cloud condensation nucleus activity of the organic component of biomass smoke particles, *Geophys. Res. Lett.*, *23*, 2141–2144, 1996.

Penkett, S. A., D. H. F. Atkins, and M. H. Unsworth, Chemical composition of the ambient aerosol in the Sudan Gezira, *Tellus*, *31*, 295–307, 1979.

Pereira, E. B., A. W. Setzer, F. Gerab, P. E. Artaxo, M. C. Pereira, and G. Monroe, Airborne measurements of aerosols from burning biomass in Brazil related to the TRACE—A experiment, *J. Geophys. Res.*, *101*, 23,983–23,992, 1996.

Pereira, J. M. C., B. S. Pereira, P. Barbosa, D. Stroppiana, M. J. P. Vasconcelos, and J.-M. Grégoire, Satellite monitoring of fire in the EXPRESSO study area during the 1996 dry season experiment: Active fires, burnt area, and atmospheric emissions, *J. Geophys. Res.*, this issue.

Pertuisot, M. H., Transfert du carbone atmosphérique dans les neiges et les pluies (in French), Ph.D. dissertation, Univ. Paris VII, Paris, 1997.

Ramdahl, T., Retene: A molecular marker of wood combustion in ambient air, *Nature*, *306*, 580–582, 1983.

Reid, J. S., P. V. Hobbs, R. J. Ferek, D. R. Blake, J. Vanderlei Martins, M. R. Dunlap, and C. Liousse, Physical, chemical, and optical properties of regional hazes dominated by smoke in Brazil, *J. Geophys. Res.*, *103*, 32,059, 1998.

Roberts, G., M. O. Andreae, W. Maenhaut, and M. T. Fernandez-Jimenez, Inorganic composition and sources of aerosols in a central African rainforest during the dry season, *J. Aerosol Sci.*, *29*, suppl. 1, S727–S728, 1998.

Rodgers, C. F., J. G. Hudson, B. Zielinska, R. L. Tanner, J. Hallet, and J. G. Watson, Cloud condensation nuclei from biomass burning, in *Global Biomass Burning: Atmospheric, Climatic and Biospheric Implications*, edited by J. S. Levine, pp. 431–438, MIT Press, Cambridge, Mass., 1991.

Saxena, P., and L. M. Hildemann, Water-soluble organics in atmospheric particles: A critical review of the literature and application of thermodynamics to identify candidate compounds, *J. Atmos. Chem.*, *24*, 57–109, 1996.

Sempéré, R., and K. Kawamura, Comparative distributions of dicarboxylic acids and related polar compounds in snow, rain and aerosols from urban atmosphere, *Atmos. Environ.*, *28*, 449–459, 1994.

Stocks, B. J., B. W. V. Wilgen, W. S. W. Trollope, D. J. McRae, J. A. Mason, F. Weirich, and A. L. F. Potgieter, Fuels and fire behavior dynamics on large-scale savanna fires in Kruger National Park, South Africa, *J. Geophys. Res.*, *101*, 23,541–23,550, 1996.

Swap, R., M. Garstang, S. A. Macko, P. D. Tyson, W. Maenhaut, P. Artaxo, P. Kallberg, and R. Talbot, The long-range transport of southern African aerosols to the tropical South Atlantic, *J. Geophys. Res.*, *101*, 23,777–23,791, 1996.

Yoboué, V., Caractéristiques physiques et chimiques des aérosols et des pluies collectés dans la savane humide de Côte d'Ivoire (in French), Ph.D. dissertation, Univ. Paul Sabatier, Toulouse, France, 1991.

Zappoli, S., et al., Inorganic, organic and their macromolecular components of fine aerosol in different areas of Europe in relation to their water solubility, *Atmos. Environ.*, *33*, 2733–2743, 1999.

H. Cachier and S. Ruellan, Laboratoire des Sciences du Climat et de l'Environnement, Bât. 12, Campus CNRS, Avenue de la Terrasse, 91198 Gif sur Yvette, France. (stéphane.ruellan@lsce.cnrs-gif.fr)

A. Gaudichet, Laboratoire Interuniversitaire des Sciences de l'Atmosphère, Faculté de Sciences, Université Paris XII, 61, Avenue du Général de Gaulle, 94010 Créteil Cedex, France.

J.-P. Lacaux, Laboratoire d'Aérologie, OMP, 14 Avenue Edouard Belin, 31400 Toulouse, France.

P. Masclet, Laboratoire d'Etude des Systèmes Atmosphériques Multiphasiques, ESIGEC, Université de Savoie, BP 1104, 73376 Le Bourget du Lac Cedex, France.

(Received March 17, 1999; revised August 2, 1999;
accepted August 4, 1999.)